

Effective Kinetic Theory for High Temperature Gauge Theories

Peter Arnold

Department of Physics, University of Virginia, Charlottesville, Virginia 22901

Guy D. Moore* and Laurence G. Yaffe

Department of Physics, University of Washington, Seattle, Washington 98195

(Dated: January 29, 2020)

Abstract

Quasiparticle dynamics in relativistic plasmas associated with hot, weakly-coupled gauge theories (such as QCD at asymptotically high temperature T) can be described by an effective kinetic theory, valid on sufficiently large time and distance scales. The appropriate Boltzmann equations depend on effective scattering rates for various types of collisions that can occur in the plasma. The resulting effective kinetic theory may be used to evaluate observables which are dominantly sensitive to the dynamics of typical ultrarelativistic excitations. This includes transport coefficients (viscosities and diffusion constants) and energy loss rates. In this paper, we show how to formulate effective Boltzmann equations which will be adequate to compute such observables to leading order in the running coupling $g(T)$ of high-temperature gauge theories [and all orders in $1/\log g(T)^{-1}$]. As previously proposed in the literature, a leading-order treatment requires including both $2 \leftrightarrow 2$ particle scattering processes as well as effective “ $1 \leftrightarrow 2$ ” collinear splitting processes in the Boltzmann equations. The latter account for nearly collinear bremsstrahlung and pair production/annihilation processes which take place in the presence of fluctuations in the background gauge field. Our effective kinetic theory is applicable not only to near-equilibrium systems (relevant for the calculation of transport coefficients), but also to highly non-equilibrium situations, provided some simple conditions on distribution functions are satisfied.

* Current address: Department of Physics, McGill University, 3600 University St., Montréal QC H3A 2T8, Canada

I. INTRODUCTION

In a hot, weakly coupled gauge theory, such as QCD at asymptotically high temperature where the running coupling $g(T)$ is small, one might hope to achieve solid theoretical control over the dynamics of the theory. To date, however, very little has been derived about the dynamics of such theories at even *leading order* in the coupling — that is, neglecting all relative corrections to the leading weak-coupling behavior which are suppressed by powers of g . For example, hydrodynamic transport properties such as shear viscosity, electrical conductivity, and flavor diffusion are not known at leading order; they have only been calculated in a “leading-log” approximation, which has relative errors of order $1/\log(g^{-1})$.¹

To study transport or equilibration processes in a hot plasma quantitatively, the most efficient approach is first to construct an effective kinetic theory which reproduces, to the required level of precision, the relevant dynamics of the underlying quantum field theory, and then apply this kinetic theory to the processes of interest. Specifically, we would like to formulate an appropriate set of Boltzmann equations which will, on sufficiently long time and distance scales, correctly describe the dynamics of typical ultrarelativistic excitations (*i.e.*, quarks and gluons) with sufficient accuracy to permit a correct leading-order evaluation of observables such as transport coefficients. Schematically, these Boltzmann equations will have the usual form,

$$(\partial_t + \mathbf{v} \cdot \nabla_{\mathbf{x}}) f = -C[f], \quad (1.1)$$

where $f = f(\mathbf{x}, \mathbf{p}, t)$ represents the phase space density of (quasi-)particles at time t , \mathbf{v} is the velocity associated with an excitation of momentum \mathbf{p} , and $C[f]$ is a spatially-local collision term that represents the rate at which particles get scattered out of the momentum state \mathbf{p} minus the rate at which they get scattered into this state. The challenge is to understand exactly what processes need to be included in the collision operator $C[f]$, and how to package them, so that the Boltzmann equation correctly reproduces the desired physics at the required level of accuracy.

To compute transport coefficients or asymptotic equilibration rates, one does not actually need a general non-equilibrium (and non-linear) kinetic theory; it is sufficient merely to have Boltzmann equations linearized in small deviations away from an equilibrium state of given temperature T .² But more generally one would like to formulate a fully non-equilibrium kinetic theory which would also be applicable to systems (such as intermediate stages of a heavy ion collision [3]) in which deviations from equilibrium are substantial and quantities such as temperature are not unambiguously defined. This will be our goal.

The domain of applicability of any kinetic theory depends on the time scales of the underlying scattering processes which are approximated as instantaneous transitions in the collision term of the Boltzmann equation. In the remainder of this introduction, we review the relevant scattering processes and associated time scales, describe the assumptions underlying our effective kinetic theory for near-equilibrium systems in which the temperature is

¹ Ref. [1] attempted to calculate the shear viscosity to next-to-leading logarithmic order [including relative corrections of order $1/\log(g^{-1})$ but neglecting $1/\log^2(g^{-1})$ effects] but, among other things, missed the “ $1 \leftrightarrow 2$ ” collinear processes described in this paper, as well as pair annihilation/creation processes which contribute even at leading-log order. The latter have been previously discussed in Ref. [2].

² See, for example, the discussion in Ref. [2].

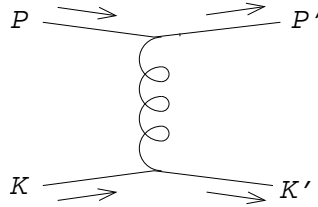


FIG. 1: Scattering of hard particles by t -channel gauge boson exchange. The straight lines could represent any type of hard charged particle, including fermions, gauge bosons, or scalars.

at least locally well-defined, and then discuss how the required conditions can be generalized to a much wider class of non-equilibrium systems.

A. Relevant scattering processes

Consider a QCD plasma at sufficiently high temperature T so that the effective coupling $g(T)$ is small.³ Quarks and gluons are well-defined quasiparticles of this system. The typical momentum (or energy) of a quark or gluon is of order T ; this will be referred to as “hard.” The number density of either type of excitation is $O(T^3)$, so that the total energy density is $O(T^4)$. Hard quarks and gluons propagate as nearly free, nearly massless excitations. Their dispersion relations receive thermal corrections which look just like an effective mass,⁴

$$\epsilon(\mathbf{p}) = \sqrt{\mathbf{p}^2 + m_{\text{th}}^2}, \quad (1.2)$$

with the thermal masses for both quarks and gluons being $O(gT)$ in size. Hence, all but a parametrically small $O(g^2)$ fraction of excitations [those with $O(gT)$ momenta] are ultra-relativistic and travel at essentially the speed of light. If $\hat{\mathbf{p}}$ denotes the unit vector in the direction of \mathbf{p} then, for hard excitations,

$$\mathbf{v}(\mathbf{p}) \equiv \frac{\partial \epsilon(\mathbf{p})}{\partial \mathbf{p}} = \hat{\mathbf{p}} [1 - O(g^2)]. \quad (1.3)$$

Scattering processes in the plasma will cause any excitation to have a finite lifetime. Imagine focusing attention on some particular excitation with a hard $O(T)$ momentum. What determines the fate of this quasiparticle? One relevant process is ordinary Coulomb scattering, depicted in Fig. 1. If the particle of interest scatters off some other excitation in the plasma with a momentum transfer \mathbf{q} , then the direction of the particle can change by an angle θ which is $O(|\mathbf{q}|/T)$. The differential scattering rate is

$$d\Gamma \sim g^4 T^3 \frac{dq}{q^3} \sim g^4 T \frac{d\theta}{\theta^3}. \quad (1.4)$$

³ For convenience of presentation, we will use the language of QCD throughout this paper. Despite this, all our discussion and results apply equally well to high temperature electroweak theory and, except for a few comments about non-perturbative non-Abelian g^2T scale physics, also to high temperature QED.

⁴ This simple form holds, up to yet higher-order corrections, provided the momenta of the excitation is large compared to the thermal mass, $|\mathbf{p}| \gg O(gT)$. Our m_{th} is often called the asymptotic thermal mass.

typical particle wavelength	T^{-1}
typical inter-particle separation	T^{-1}
Debye screening length	$(gT)^{-1}$
inverse thermal mass	$(gT)^{-1}$
mean free path: small-angle scattering ($\theta \sim g$, $q \sim gT$)	$(g^2T)^{-1}$
mean free path: very-small-angle scattering ($\theta \sim g^2$, $q \sim g^2T$)	$(g^2T)^{-1}$
duration (formation time) of “1 \leftrightarrow 2” collinear processes	$(g^2T)^{-1}$
non-perturbative magnetic length scale for colored fluctuations	$(g^2T)^{-1}$
mean free path: large-angle scattering ($\theta \sim 1$, $q \sim T$)	$(g^4T)^{-1}$
mean free path: hard “1 \leftrightarrow 2” collinear processes	$(g^4T)^{-1}$

TABLE I: Parametric dependence of various length scales for a weakly-coupled ultrarelativistic equilibrium plasma. Estimates for mean free paths apply to typical (hard) particles, with θ and q denoting the deflection angle and momentum transfer, respectively. The non-perturbative magnetic physics scale of $(g^2T)^{-1}$ for colored fluctuations applies only to non-Abelian gauge theories.

This form holds provided $q \gtrsim O(gT)$. Below this scale, Debye screening (and Landau damping) in the plasma soften the small angle divergence of the bare Coulomb interaction.

Consequently, the rate for a single large angle scattering with $O(T)$ momentum transfer is $O(g^4T)$, while the rate for small angle scattering with $O(gT)$ momentum transfer is $O(g^2T)$. For later use, let $\tau_g = 1/(g^2T)$ denote the characteristic small angle mean free time, and $\tau_* = 1/(g^4T)$ the characteristic large angle mean free time,⁵ also known as the transport

⁵ Actually, because small angle scatterings are individually more probable than large angle scatterings, a particle can undergo $N_g \sim 1/g^2$ small angle scatterings, each with $\theta = O(g)$, during a time of order $N_g \tau_g \sim 1/(g^4T)$ — the same as the time for a single $q = O(T)$ scattering. A succession of this many uncorrelated small angle scatterings will result in a net deflection of order $N_g^{1/2} \theta = O(1)$. Hence, a large deflection in the direction of a particle is equally likely to be the result of many small angle scatterings or a single large angle scattering. In fact, the multiplicity of possible combinations of scatterings with angles between $\theta \sim g$ and $\theta \sim 1$ leads to a logarithmic enhancement in the large angle scattering rate, or a logarithmic decrease of the large angle mean free path, so that $\tau_* \sim [g^4T \log(1/g)]^{-1}$. In this paper, we will ignore such logarithmic factors when making parametric estimates and simply write $\tau_* \sim 1/g^4T$. Nevertheless, it is important to keep in mind that contributions to τ_* come from the entire range of scatterings from $\theta \sim g$ to $\theta \sim 1$, which corresponds to momentum transfers from $q \sim gT$ to $q \sim T$.

Yet softer momentum transfers are screened in the plasma and do not affect τ_* at the order of interest. For instance, the mean free path for very-small-angle scattering with $\theta \sim g^2$ (corresponding to momentum transfers of order g^2T) is only $\tau_{g^2} \sim 1/g^2T$ and is not enhanced over τ_g . Over the time $\tau_* \sim 1/g^4T$, there can thus be only $N_{g^2} \sim 1/g^2$ independent very-soft scatterings, which will only contribute a net deflection of order $\Delta\theta \sim (N_{g^2})^{1/2} g^2 \sim g$ to the $O(1)$ deflection caused by other processes. Consequently, the large angle scattering time τ_* is insensitive to non-perturbative magnetic physics in the plasma associated with very soft momentum transfers of order g^2T .

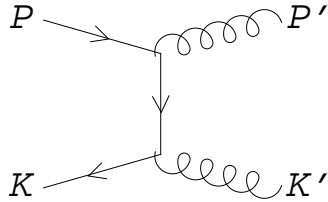


FIG. 2: *t*-channel diagram for $q\bar{q} \rightarrow gg$.

mean free time. Neither time has a precise, quantitative definition; these quantities will only be used in parametric estimates. The small angle mean free time τ_g is [to within a factor of $O(\log g^{-1})$] the same as the color coherence time of an excitation — this is the longest time scale over which it makes sense to think of an excitation has having a definite (non-Abelian) color [4–7]. These scales are summarized in Table I.

It is also important to consider processes which change the *type* of an excitation. Consider, for example, the conversion of a quark of momentum \mathbf{p} into a gluon of nearly the same momentum by the soft $q\bar{q} \rightarrow gg$ process, depicted in Fig. 2, with momentum transfer $\mathbf{q} \sim gT$. The mean free path for this process (or its time-reverse) is $O[1/(g^4 T)]$, just like the large angle scattering time τ_* . As a result, such *t*-channel quark exchange processes are equally important as gluon exchange for quasiparticle dynamics, and must be correctly included even in leading-log evaluations of transport coefficients [2].

Crossed *s*-channel versions of Figs. 1 and 2, namely quark-antiquark annihilation and creation via a single virtual gluon, and gluon-Compton scattering, also proceed at $O(g^4 T)$ rates. Consequently, these processes must also be included in a leading-order treatment of quasiparticle dynamics.⁶ Henceforth, whenever we refer to $2 \leftrightarrow 2$ particle processes, we will mean all possible crossings of Figs. 1 and 2 in which two excitations turn into two excitations.

In addition to the $2 \leftrightarrow 2$ particle processes of Figs. 1 and 2, hard quasiparticles in the plasma can also undergo processes in which they effectively split into two different, nearly collinear, hard particles. Such processes cannot occur (due to energy-momentum conservation) in vacuum, but they become kinematically allowed when combined with a soft exchange involving some other excitation in the plasma. A specific example is the bremsstrahlung process depicted in the upper part of Fig. 3. Here, one hard quark undergoes a soft ($\mathbf{q} \sim gT$) collision with another and splits into a hard quark plus a hard gluon, each of which carry an $O(1)$ fraction of the hard momentum of the original quark and both of which travel in the same direction as the original quark to within an angle of $O(g)$. The mean free path for this process, as well as the near-collinear pair production process also shown in Fig. 3, turns out to be $O[1/(g^4 T)]$, which is once again the same order as the large angle scattering time τ_* .⁷

⁶ These *s*-channel processes do not have the logarithmic enhancement mentioned in footnote 5, and so do not contribute to transport coefficients at leading-log order, but do contribute at next-to-leading log order.

⁷ See, for example, Ref. [8] as well as the discussion of the closely related case of photon emission in Refs. [9, 10]. More careful analysis shows that the rates of these near-collinear processes do not have the logarithmic enhancement of the large angle scattering rate discussed in footnote 5. Therefore these near-collinear processes do not contribute to transport coefficients at leading-log order but must be included at next-to-leading log order.

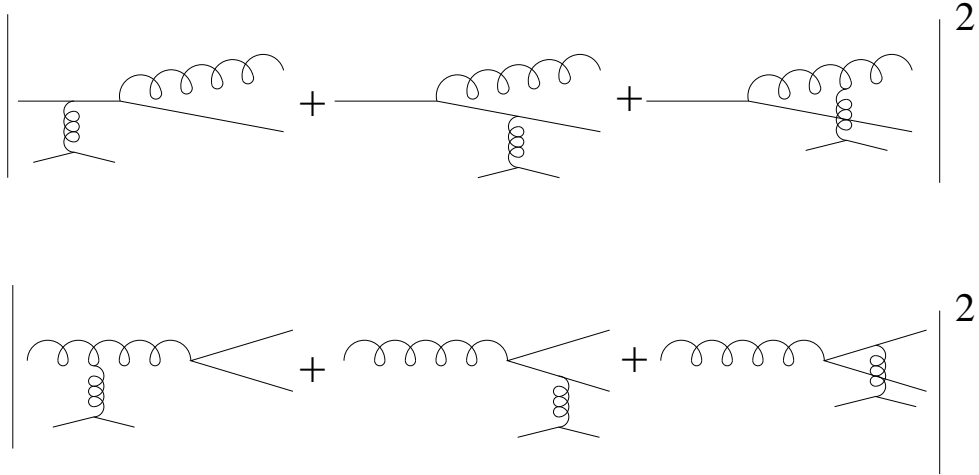


FIG. 3: Simplest examples of near-collinear processes which contribute at leading order. The upper diagrams depict hard, nearly collinear gluon bremsstrahlung accompanying a soft gluon exchange between hard particles. The lower diagrams show the conversion of a hard gluon into a nearly collinear quark-antiquark pair when accompanied by a soft exchange with another excitation in the plasma.

There is an important difference between these near-collinear processes and the $2 \leftrightarrow 2$ particle processes of Figs. 1 and 2. The intermediate propagator in the diagrams of Fig. 3 which connects the “splitting” vertex with the soft exchange has a small $O(g^2 T^2)$ virtuality. Physically, this means that the time duration of the near-collinear processes (also known as the scattering time or formation time) is of order $1/g^2 T$, which is the same as the mean free time τ_g for small-angle elastic collisions in the plasma. As a result, additional soft collisions are likely to occur during the splitting process and can disrupt the coherence between the nearly collinear excitations. This is known as the Landau-Pomeranchuk-Migdal (LPM) effect. Since the time between soft scatterings is comparable to the time duration of the emission process, multiple soft scatterings cannot be treated as independent classical events, but must be evaluated fully quantum mechanically. In other words, including the interference between different $N + 1 \rightarrow N + 2$ amplitudes, such as depicted in Fig. 4, is required to evaluate correctly the rate for near-collinear splitting at leading order. We will refer to these processes collectively as “ $1 \rightarrow 2$ ” processes where the $1 \rightarrow 2$ refers to the nearly collinear splitting particles and the quotes are a reminder that there are other hard particles participating in the process via multiple soft gluon exchanges. Of course, the inverse “ $2 \rightarrow 1$ ” processes, in which two nearly collinear excitations fuse into one, are also required for detailed balance. The evaluation of the rate of these “ $1 \leftrightarrow 2$ ” near-collinear processes in an equilibrium ultrarelativistic plasma, complete to leading order, is discussed in Ref. [8],⁸ which derives a two-dimensional linear integral equation whose solution determines the leading order rate.

Having realized that near-collinear “ $1 \leftrightarrow 2$ ” processes are just as important to the fate of a quasiparticle as $2 \leftrightarrow 2$ particle processes, one might wonder if there are any further relevant processes which occur at an $O(g^4 T)$ rate and hence compete with the processes just

⁸ See also Refs. [9, 11] and references therein.

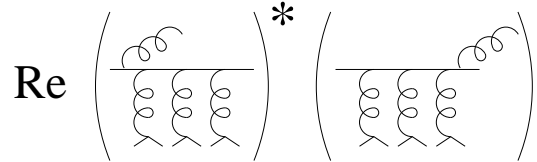


FIG. 4: Examples of interference terms involving multiple scatterings that also contribute to hard-gluon bremsstrahlung at leading order.

discussed. We will argue in section VI that this is not the case.

In summary, a typical hard excitation travels a distance of order $\tau_* \sim 1/(g^4 T)$ before it either experiences a large angle scattering, converts into another type of excitation, splits into two nearly collinear hard excitations, or merges with another nearly collinear excitation. These different ‘‘fates’’ are all comparably likely [up to factors of $O(\log g^{-1})$]. During the transport mean free time τ_* , the excitation will experience many soft scatterings each of which can completely reorient the color of the quasiparticle, but only change its momentum by a small $O(gT)$ amount.

B. Kinetic theory domain of validity — near-equilibrium systems

A near-equilibrium system is one in which the phase space distribution can be written as an equilibrium distribution $n(\mathbf{p})$ plus a small perturbation $\delta f(\mathbf{x}, \mathbf{p})$. However, we wish to include situations where the system is close to local rather than global equilibrium, so that equilibrium parameters like temperature may vary slowly with \mathbf{x} . We will therefore define a near-equilibrium system to be one where distribution functions can be written in the form

$$f(\mathbf{x}, \mathbf{p}) = n(\mathbf{p}; T(\mathbf{x}), \mathbf{u}(\mathbf{x}), \mu(\mathbf{x})) + \delta f(\mathbf{x}, \mathbf{p}), \quad (1.5)$$

where $n(\mathbf{p}; T, \mathbf{u}, \mu)$ denotes an equilibrium distribution (Bose or Fermi, as appropriate) with temperature T , flow velocity \mathbf{u} , and optionally one or more chemical potentials μ , provided: (i) the parameters $T(\mathbf{x})$, $\mathbf{u}(\mathbf{x})$, and $\mu(\mathbf{x})$ do not vary significantly over distances (or times) of order $1/g^4 T$, the large angle mean free path,⁹ and (ii) everywhere, $\delta f(\mathbf{p}, \mathbf{x}) \ll f(\mathbf{p}, \mathbf{x})$.

In the case of near-equilibrium systems, we can now summarize the conditions upon which our effective kinetic theory is based.

1. As already indicated, we assume that the theory is weakly coupled on the scale of the temperature, $g(T) \ll 1$. Consequently, there is a parametrically large separation between the different scales shown in Table I.
2. We assume that all zero-temperature mass scales (*i.e.*, Λ_{QCD} and current quark masses) are negligible compared to the $O(gT)$ scale of thermal masses.¹⁰

⁹ This condition should be understood as applying in a frame which is slowly moving relative to the local rest frame of the fluid at point \mathbf{x} .

¹⁰ For hot electroweak theory, the required condition is that the Higgs condensate be small compared to the temperature, $v(T) \ll T$, so that the condensate-induced mass of the W -boson is negligible compared to its thermal mass.

3. Any kinetic theory can only be valid on time scales which are large compared to the duration of the scattering processes which are approximated as instantaneous inside the collision term of the Boltzmann equation. Since the formation time of near-collinear splitting processes is order $1/(g^2 T)$, this means we must assume that the space-time variation of the deviation from local equilibrium $\delta f(\mathbf{x}, \mathbf{p})$ is small on the scale of $1/(g^2 T)$. [Note that we've already assumed a stronger condition on the spacetime variation of the local equilibrium part of distributions, $n(\mathbf{p}; T(\mathbf{x}), \mathbf{u}(\mathbf{x}), \mu(\mathbf{x}))$.]
4. We will assume that hard particle distribution functions $\delta f(\mathbf{x}, \mathbf{p})$ have smooth dependence on momentum \mathbf{p} and do not vary significantly with changes in momentum comparable to the $O(gT)$ size of thermal masses. [Again, this is automatic for the local equilibrium part of distributions.] This condition will allow us to simplify our treatment of distribution functions for near-collinear “ $1 \leftrightarrow 2$ ” processes.
5. Finally, we assume that the observables of ultimate interest are dominantly sensitive to the dynamics of hard excitations, are smooth functions of the momenta of these excitations, do not depend on the spin of excitations, and are gauge invariant. Excluding spin-dependent observables is primarily a matter of convenience, and will allow us to use spin-averaged effective scattering rates.¹¹ Considering color-dependent observables would be senseless in an effective theory which is only applicable on spatial scales large compared to the $1/(g^2 T)$ color coherence length.

C. Kinetic theory domain of validity — non-equilibrium case

It is impossible for any effective kinetic theory to be valid for all possible choices of phase space distribution functions. There will always exist sufficiently pathological initial states which are outside the domain of applicability of any kinetic theory. Describing the domain of applicability therefore requires a suitable characterization of acceptable distribution functions. In a general non-equilibrium setting, we will define “reasonable” distribution functions to be those which support a separation of scales similar to the weakly-coupled equilibrium case. That is, the momenta of relevant excitations must be parametrically large compared to medium-dependent corrections to dispersion relations or to the inverse Debye screening length. Furthermore, the phase space density of excitations must not be so large as to drive the dynamics, on these scales, into the non-perturbative regime.

There are potentially many more relevant scales one may need to distinguish in a non-equilibrium setting. In particular, in place of the single hard scale T that characterizes the momenta of typical excitations in equilibrium, one may need to consider at least three relevant scales, which we shall refer to as the typical momenta of (i) primaries, (ii) screeners, and (iii) scatterers. By “primaries,” we mean the particles whose evolution we are explicitly

¹¹ If this condition is not met, distribution functions become density matrices in spin space, and the Boltzmann equation must be replaced by a generalization known as a Waldmann-Snider equation [12]. (See also the discussion in Ref. [4] for the analogous case of color-dependent density matrices.) We assume spin-independence to avoid needlessly complicating this paper, and because we are not aware of physically interesting problems in hot gauge theories where strong spin polarization is relevant.

interested in following with the Boltzmann equation. These might be the particles which dominate the energy of the system (as in the intermediate stages of bottom-up thermalization [3]), they might be particles which dominate transport of some charge of the system we are following, or whatever. These excitations may or may not overlap with the next two categories. The “screeners” are those particles whose response to electric and magnetic fields dominates the screening effects and hard thermal masses in the medium. That is, they have momenta comparable to the momentum scale at which hard thermal-loop (HTL) self-energies receive their dominant contribution. (Explicit formulas for HTL self-energies will be reviewed in Section IV.) Finally, the “scatterers” are those particles which generate the soft background of gauge fields off of which the primaries scatter in soft collisions. As a pictorial example, consider Figs. 1, 3, and 4. The lines entering on the top are primaries, the lines entering on the bottom are scatterers, and the screeners are not shown explicitly but are the particles in the hard thermal loops that are implicitly summed in the soft, exchanged gluon lines.

To formulate the conditions under which our Boltzmann equations will be valid, it will be helpful to define the following two integrals involving the distribution function of a particular species (gluon, quark, or antiquark) of quasiparticles,

$$\mathcal{J}(\mathbf{x}) \equiv \int \frac{d^3\mathbf{p}}{(2\pi)^3} \frac{f(\mathbf{p}, \mathbf{x})}{|\mathbf{p}|}. \quad (1.6)$$

$$\mathcal{I}(\mathbf{x}) \equiv \frac{1}{2} \int \frac{d^3\mathbf{p}}{(2\pi)^3} f(\mathbf{p}, \mathbf{x}) [1 \pm f(\mathbf{p}, \mathbf{x})], \quad (1.7)$$

As usual upper signs refer to bosons and lower signs to fermions. In equilibrium, the ratio \mathcal{I}/\mathcal{J} is precisely the temperature T .

Corrections to the ultrarelativistic dispersion relation for quasiparticles will be seen to involve the quantity $\mathcal{J}(\mathbf{x})$; the square of medium-dependent effective masses will be of order $g^2 \mathcal{J}$. So the momentum dominating this integral defines the typical momentum of screeners which we will denote by p_{screen} , and

$$m_{\text{eff}} \sim g\sqrt{\mathcal{J}} \quad (1.8)$$

is the characteristic size of effective masses. This reduces to the gT scale in the near-equilibrium case. Momenta large compared to m_{eff} will be referred to as “hard.”

The integral $\mathcal{I}(\mathbf{x})$ will appear as an effective density of scatterers which generate soft background gauge field fluctuations. The momentum scale which dominates this integral is, by definition, the characteristic momentum of scatterers, p_{scatter} . The mean free time between small-angle scatterings (with momentum transfer of order m_{eff}) scales as¹²

$$\tau_{\text{soft}} \sim \frac{m_{\text{eff}}^2}{g^4 \mathcal{I}}. \quad (1.9)$$

¹² Initial and final state factors for the scatterer appear in this expression inside the integral \mathcal{I} , given by Eq. (1.7). Some readers may wonder whether there should be analogous initial and final state factors for the primary excitation. To be more precise, τ_{soft} represents the inverse of the contribution to the thermal width of quasiparticles due to soft scattering. This part of the width does not contain statistical factors for the primaries. The scale τ_{soft} characterizes the time scale for the decay of quasiparticle excitations. Equivalently, it is the relaxation time of fluctuations in the occupancy of a hard mode due to soft scattering.

This generalizes the $1/(g^2 T)$ small angle mean free time in the near-equilibrium case.

Let p_{primary} denote the characteristic primary momenta of interest, and let p_{hard} denote the minimum of p_{scatter} , p_{screen} , and p_{primary} . As we shall review in section V B, the formation time of near-collinear bremsstrahlung or annihilation processes involving a primary excitation behaves (up to logarithms) as

$$t_{\text{form}} \sim \frac{p_{\text{primary}}}{N_{\text{form}} m_{\text{eff}}^2}, \quad (1.10)$$

where

$$N_{\text{form}} \sim \left[1 + \frac{p_{\text{primary}}}{m_{\text{eff}}^2 \tau_{\text{soft}}} \right]^{1/2} \quad (1.11)$$

represents the typical number of soft collisions occurring during a single near-collinear “ $1 \leftrightarrow 2$ ” process. (In other words, N_{form} is parametrically either 1 or $[p_{\text{primary}}/(m_{\text{eff}}^2 \tau_{\text{soft}})]^{1/2}$, depending on whether p_{primary} is small or large compared to $m_{\text{eff}}^2 \tau_{\text{soft}}$.)

Since distribution functions may vary in space or time, all these scales are really local and may vary from point to point in spacetime. However, we will assume that distribution functions are suitably slowly varying in space and time. The following discussion should be understood as applying in the vicinity of any particular point \mathbf{x} in the system.

The key assumptions we will make are:

1. The species dependence of the above scales is not parametrically large. In particular, ratios of the effective masses of different species are $O(1)$. This assumption is a matter of convenience, but relaxing it would significantly complicate the discussion.
2. The momenta of primaries, scatterers, and screeners are all large compared to medium-dependent effective masses. A large separation of scales is essential to our analysis, and implies that all relevant excitations are highly relativistic. To make parametric estimates, we will assume that

$$m_{\text{eff}}/p_{\text{hard}} \lesssim O(g^\alpha) \quad (1.12)$$

for some positive exponent α . [For instance, $m_{\text{eff}}/p_{\text{hard}}$ was $O(g)$ in our previous discussion of near-equilibrium physics.]

3. The effective mass m_{eff} must be large compared to the small-angle scattering rate τ_{soft}^{-1} , as well as to zero-temperature mass scales (Λ_{QCD} and quark masses).
4. Distribution functions of scatterers and screeners do not vary significantly with parametrically small changes in the direction of propagation of excitations. For example, distributions cannot be so highly anisotropic that the directions of screeners or scatterers all lie within an $O(g)$ angle of each other. This assumption prevents potential instabilities [13] and simplifies the analysis.
5. All distribution functions have negligible variation over spacetime regions whose size equals the formation time t_{form} of near-collinear processes involving primary excitations. This assumption is essential for our treatment of near-collinear processes.

6. Distribution functions, for hard momenta, have smooth dependence on momentum and do not vary significantly with $O(m_{\text{eff}})$ changes in momentum. [This assumption is implicit in various non-equilibrium HTL results which we will take from the literature.] For momenta of order p_{primary} , we further assume that distributions do not vary significantly with an $O(N_{\text{form}}^{1/2} m_{\text{eff}})$ change in momentum, which represents the typical total momentum transfer due to the N_{form} soft collisions occurring during a near-collinear “ $1 \leftrightarrow 2$ ” process.
7. Distribution functions are not non-perturbatively large for momenta $p \gtrsim O(m_{\text{eff}})$. Specifically, for bosonic species we will assume that $f(\mathbf{p}, \mathbf{x})$ is parametrically small compared to $1/g^2$. (Fermionic distributions can never be parametrically large.) As discussed below, this inequality is actually a consequence of condition 2.
8. Distribution functions are not spin-polarized. Once again, this condition is a matter of convenience. But the consistency of this assumption is now a non-trivial issue since we are not requiring distribution functions to be isotropic in momentum space. In a general (rotationally invariant) theory, it is quite possible for a medium with anisotropic distribution functions to generate medium-dependent self-energy corrections which lead to spin or polarization dependent dispersion relations, implying spin-dependent propagation of quasiparticles. In such a theory, initially unpolarized distribution functions would not remain unpolarized. This point will be discussed further in section IV, where we will see that in hot gauge theories (at the level of precision relevant for our leading-order kinetic theory) unpolarized but anisotropic distribution functions do not generate birefringent quasiparticle dispersion relations.
9. Distribution functions are color singlets. Attempting to incorporate colored distribution functions would be inconsistent, since the color coherence time is comparable or shorter than the formation time of the “ $1 \leftrightarrow 2$ ” processes which will be treated as instantaneous in this effective kinetic theory.
10. Observables of interest are dominantly sensitive to the dynamics of excitations with momenta of order p_{primary} , are smooth functions on phase space, are gauge invariant, and are spin independent.

The most important restrictions are the scale-separation condition 2 and the effective mass condition 3. They have numerous consequences, including condition 7, as explained below.

Let \bar{f}_p denote the average phase space density for excitations with momenta of order p . First note that the definition of p_{screen} as the momentum which dominates the integral \mathcal{J} (1.6) implies that

$$p^2 \bar{f}_p \lesssim p_{\text{screen}}^2 \bar{f}_{p_{\text{screen}}} \sim \mathcal{J}, \quad (1.13)$$

for any momentum p . For momenta p which are parametrically different from p_{screen} , the above inequality (\lesssim) is actually a strong inequality (\ll) (or else p_{screen} will not be the scale which dominates \mathcal{J}). From (1.13) and definition (1.8), one has

$$p^2 \bar{f}_p \lesssim m_{\text{eff}}^2/g^2. \quad (1.14)$$

For hard momenta $p \gtrsim p_{\text{hard}}$, condition 2 [$m_{\text{eff}}^2/p^2 \lesssim O(g^{2\alpha})$] thus implies that

$$\bar{f}_p \lesssim O(g^{2\alpha-2}), \quad (1.15)$$

which is a strengthened version of condition 7. For soft momenta, such as $p \sim m_{\text{eff}}$, which are parametrically smaller than p_{scatter} by condition 2, the inequality (1.14) becomes strong, $p^2 \bar{f}_p \ll m_{\text{eff}}^2/g^2$. We can then generally conclude that for momenta $p \gtrsim m_{\text{eff}}$, the phase space density is perturbative,

$$f_p \ll O(g^{-2}). \quad (1.16)$$

In order for any Boltzmann equation to be valid, the duration of scattering events (which are treated as instantaneous in the Boltzmann equation) must be small compared to the typical time between scatterings. For $2 \leftrightarrow 2$ collisions, the largest relevant scattering duration is $1/m_{\text{eff}}$ [for soft scatterings with $O(m_{\text{eff}})$ momentum transfer] and the smallest relevant mean free time is the small-angle scattering time (1.9). Hence, the condition 3 requirement that $m_{\text{eff}} \tau_{\text{soft}} \gg 1$ is needed for the validity of kinetic theory. If the density of scatterers is not parametrically small, so that $\bar{f}_{p_{\text{scatter}}}[1 \pm \bar{f}_{p_{\text{scatter}}}]$ is $O(1)$ or larger, then this inequality automatically holds since Eqs. (1.13) and (1.15) imply¹³

$$m_{\text{eff}} \tau_{\text{soft}} \sim \frac{\mathcal{J}^{3/2}}{g \mathcal{I}} \sim \frac{\bar{f}_{p_{\text{screen}}}^{3/2} p_{\text{screen}}^3}{g \bar{f}_{p_{\text{scatter}}}^2 p_{\text{scatter}}^3} \gtrsim (g^2 \bar{f}_{p_{\text{scatter}}})^{-1/2} \gtrsim O(g^{-\alpha}). \quad (1.17)$$

But the more general condition 3 determines the limit of applicability of kinetic theory for dilute systems.

In order to regard excitations as having well-defined energies and momenta, their de Broglie wavelengths must also be small compared to the mean time between scatterings. The longest relevant de Broglie wavelength is $1/p_{\text{hard}}$, so the validity of kinetic theory requires that $p_{\text{hard}} \tau_{\text{soft}} \gg 1$. But this automatically follows from conditions 2 and 3.

Condition 6, requiring smoothness of distribution functions in momentum space, prevents applications of our effective theory to cold degenerate quark matter. This condition implies that the temperature (for near-equilibrium systems) must be large compared to $g p_{\text{fermi}}$ and hence, for weak coupling, lies far outside the temperature region in which color superconductivity occurs.

The remainder of this paper is organized as follows. Section II presents the structure of the effective kinetic theory. The effective scattering amplitudes characterizing $2 \leftrightarrow 2$ processes are discussed in section III. These quasiparticle scattering amplitudes depend on medium-dependent self-energies, which are the subject of section IV. The appropriate formulation of effective transition rates for near-collinear “ $1 \leftrightarrow 2$ ” processes is described in section V. Section VI discusses the validity of our effective kinetic theory at greater length, including possible double counting problems in our effective collision terms, and potential contributions of omitted scattering processes. We argue that neither of these concerns are an issue. This section also briefly mentions open problems associated with extending our effective kinetic theory beyond leading order. Two brief appendices follow. One summarizes simplifications to the formulas in the main text that can be made in the special case of isotropic distribution functions, and the other discusses the connection between the formulas for $1 \leftrightarrow 2$ scattering presented in section V and the results for the total gluon emission rate discussed in Ref. [8].

¹³ This estimate assumes that some of the relevant scatterers are bosons, which might have parametrically large distributions. If the only relevant scatterers are fermions, then one finds $m_{\text{eff}} \tau_{\text{soft}} \gtrsim O(1/g)$.

II. THE EFFECTIVE KINETIC THEORY

Our effective kinetic theory will include all $2 \leftrightarrow 2$ processes as well as effective collinear “ $1 \leftrightarrow 2$ ” processes. The Boltzmann equations are,

$$(\partial_t + \hat{\mathbf{p}} \cdot \nabla_{\mathbf{x}}) f_s(\mathbf{x}, \mathbf{p}, t) = -C_s^{2 \leftrightarrow 2}[f] - C_s^{“1 \leftrightarrow 2”}[f], \quad (2.1)$$

where the label s denotes the species of excitation (gluon, up-quark, up-antiquark, down-quark, down-antiquark, *etc.*). Since we have assumed that distributions are not spin or color polarized, we do not decorate distribution functions with any spin or color label. However it should be understood that $f_s(\mathbf{x}, \mathbf{p}, t)$ represents the phase space density of a single helicity and color state of type s quasiparticles.¹⁴

Schematically, the overall structure of our Boltzmann equations is similar to that outlined by Baier, Mueller, Schiff, and Son [3] in their treatment of the late stages of their “bottom-up” picture of thermalization in heavy ion collisions, but our formulation of the details of the collision terms will be guided by our goal of providing a treatment which is complete at leading order. As will be discussed below, this requires a consistent treatment of both screening and LPM suppression of near-collinear processes.

The elastic $2 \leftrightarrow 2$ collision term for a given species a has a conventional form,

$$C_a^{2 \leftrightarrow 2}[f] = \frac{1}{4|\mathbf{p}|\nu_a} \sum_{bcd} \int_{\mathbf{k}\mathbf{p}'\mathbf{k}'} |\mathcal{M}_{cd}^{ab}(\mathbf{p}, \mathbf{k}; \mathbf{p}', \mathbf{k}')|^2 (2\pi)^4 \delta^{(4)}(P + K - P' - K') \times \left\{ f_a(\mathbf{p}) f_b(\mathbf{k}) [1 \pm f_c(\mathbf{p}')] [1 \pm f_d(\mathbf{k}')] - f_c(\mathbf{p}') f_d(\mathbf{k}') [1 \pm f_a(\mathbf{p})] [1 \pm f_b(\mathbf{k})] \right\}. \quad (2.2)$$

We have introduced ν_s as the number of spin times color states for species s . (So ν_s equals 6 for each quark or antiquark, and 16 for gluons.) Capital letters denote 4-vectors. The on-shell 4-momenta appearing inside the delta-function are to be understood as null vectors,

$$P^0 \equiv |\mathbf{p}|, \quad \text{etc.} \quad (2.3)$$

We are using $\int_{\mathbf{p}}$ to denote Lorentz invariant momentum integration,

$$\int_{\mathbf{p}} \cdots \equiv \int \frac{d^3 \mathbf{p}}{2|\mathbf{p}| (2\pi)^3} \cdots. \quad (2.4)$$

The first term in curly braces in (2.2) is a loss term, and the second is a gain term. \mathcal{M}_{cd}^{ab} denotes an effective scattering amplitude for the process $ab \leftrightarrow cd$, defined with a relativistic normalization for single particle states; its square, $|\mathcal{M}_{cd}^{ab}|^2$, should be understood as summed, not averaged, over the spins and colors of all four excitations (hence the prefactor of $1/\nu_a$). The initial factor of $1/(4|\mathbf{p}|)$ is a combination of a final (or initial) state symmetry factor¹⁵ of $\frac{1}{2}$ together with the $1/(2|\mathbf{p}|)$ from the relativistic normalization of the scattering amplitude.

¹⁴ Since our effective theory describes typical hard excitations, gluons are to be regarded as having only two transverse polarizations. There is a longitudinal branch of the gluon dispersion relation in a hot plasma, but the spectral density of longitudinal excitations is exponentially small for hard momenta. Hence, these collective excitations may be completely ignored for our present purposes.

¹⁵ When the species c and d are identical, a symmetry factor is required. When they are distinct, the final state is double-counted in the sum \sum_{cd} over species. Hence a factor of $\frac{1}{2}$ is needed in either case.

Symmetry under time-reversal and particle interchange imply that

$$|\mathcal{M}_{cd}^{ab}(\mathbf{p}, \mathbf{k}; \mathbf{p}', \mathbf{k}')|^2 = |\mathcal{M}_{dc}^{ab}(\mathbf{p}, \mathbf{k}; \mathbf{k}', \mathbf{p}')|^2 = |\mathcal{M}_{cd}^{ba}(\mathbf{k}, \mathbf{p}; \mathbf{p}', \mathbf{k}')|^2 = |\mathcal{M}_{ab}^{cd}(\mathbf{p}', \mathbf{k}'; \mathbf{p}, \mathbf{k})|^2, \quad (2.5)$$

etc. The effective scattering amplitude will itself be a functional of the distribution functions, since the density of other particles in the plasma determines screening lengths which affect the amplitude for soft scattering. This will be discussed explicitly in the next section.

As Eq. (2.3) makes explicit, we have neglected medium-dependent corrections to quasiparticle dispersion relations in the overall kinematics of the collision terms, and in the particle velocity appearing in the convective derivative on the left side of the Boltzmann equation (2.1). Given our assumed separation of scales, these are relative $O(g^{2\alpha})$ perturbations to the energy or velocity of a hard quasiparticle. Because we have assumed that distribution functions and observables are smooth functions on phase space, including (or excluding) these medium-dependent dispersion relation corrections will only affect subleading corrections to observables of interest. (This is discussed further in sections III and VI.)

Now consider “ $1 \leftrightarrow 2$ ” processes. If isolated $1 \leftrightarrow 2$ processes are kinematically allowed by the effective thermal masses of the particles involved, and if there were no need to consider $1 + N \leftrightarrow 2 + N$ processes, then the appropriate $1 \leftrightarrow 2$ collision term would have a form completely analogous to the $2 \leftrightarrow 2$ collision term:

$$\begin{aligned} C_a^{1 \leftrightarrow 2}[f] &= \frac{1}{4|\mathbf{p}|\nu_a} \sum_{b,c} \int_{\mathbf{p}'\mathbf{k}'} |\mathcal{M}_{bc}^a(\mathbf{p}; \mathbf{p}', \mathbf{k}')|^2 (2\pi)^4 \delta^{(4)}(P - P' - K') \\ &\quad \times \left\{ f_a(\mathbf{p})[1 \pm f_b(\mathbf{p}')][1 \pm f_c(\mathbf{k}')] - f_b(\mathbf{p}')f_c(\mathbf{k}')[1 \pm f_a(\mathbf{p})] \right\} \\ &+ \frac{1}{2|\mathbf{p}|\nu_a} \sum_{b,c} \int_{\mathbf{k}\mathbf{p}'} |\mathcal{M}_{ab}^c(\mathbf{p}'; \mathbf{p}, \mathbf{k})|^2 (2\pi)^4 \delta^{(4)}(P + K - P') \\ &\quad \times \left\{ f_a(\mathbf{p})f_b(\mathbf{k})[1 \pm f_c(\mathbf{p}')] - f_c(\mathbf{p}')[1 \pm f_a(\mathbf{p})][1 \pm f_b(\mathbf{k})] \right\}. \end{aligned} \quad (2.6)$$

With strictly massless kinematics, it is impossible to satisfy both energy and momentum conservation in a $1 \leftrightarrow 2$ particle process unless all particles are exactly collinear. For small masses (compared to the energies of the primaries), the particles will be very nearly collinear. One could then integrate over the small transverse momenta associated with the splitting to recast the collision term in the form

$$\begin{aligned} C_a^{“1 \leftrightarrow 2”}[f] &= \frac{(2\pi)^3}{2|\mathbf{p}|^2\nu_a} \sum_{b,c} \int_0^\infty dp' dk' \delta(|\mathbf{p}| - p' - k') \gamma_{bc}^a(\mathbf{p}; p' \hat{\mathbf{p}}, k' \hat{\mathbf{p}}) \\ &\quad \times \left\{ f_a(\mathbf{p})[1 \pm f_b(p' \hat{\mathbf{p}})][1 \pm f_c(k' \hat{\mathbf{p}})] - f_b(p' \hat{\mathbf{p}})f_c(k' \hat{\mathbf{p}})[1 \pm f_a(\mathbf{p})] \right\} \\ &+ \frac{(2\pi)^3}{|\mathbf{p}|^2\nu_a} \sum_{b,c} \int_0^\infty dk dp' \delta(|\mathbf{p}| + k - p') \gamma_{ab}^c(p' \hat{\mathbf{p}}; \mathbf{p}, k \hat{\mathbf{p}}) \\ &\quad \times \left\{ f_a(\mathbf{p})f_b(k \hat{\mathbf{p}})[1 \pm f_c(p' \hat{\mathbf{p}})] - f_c(p' \hat{\mathbf{p}})[1 \pm f_a(\mathbf{p})][1 \pm f_b(k \hat{\mathbf{p}})] \right\}, \end{aligned} \quad (2.7)$$

where we have ignored the small deviations from exact collinearity when evaluating the distribution functions. The factor of $\gamma_{bc}^a(\mathbf{p}; p' \hat{\mathbf{p}}, k' \hat{\mathbf{p}})$ in the integrand is simply a way of parameterizing the differential rate $d\Gamma/dp dp' dk d\Omega_{\hat{\mathbf{p}}}$ for an $a \rightarrow bc$ splitting processes, integrated

over transverse momenta, excluding distribution functions and the longitudinal-momentum conserving δ -function.

Any nearly-collinear “ $1 \leftrightarrow 2$ ” process, now including $1 + N \leftrightarrow 2 + N$ soft scattering with emission events, can be cast into the general form of (2.7). The only difference is that the differential splitting/joining rates γ_{bc}^a will now implicitly depend on the distribution functions for the N scatterers. All of the phase space integrations for those scatterers, plus the summation over N , will be packaged into γ_{bc}^a . The appropriate values of the splitting rates γ_{bc}^a will be determined simply by requiring that the collision term (2.7) reproduce previous results in the literature for the rates of “ $1 \leftrightarrow 2$ ” processes.

In the collision term (2.7), we have written the momenta of the splitting (or joining) particles as though they were exactly collinear and as though their energy was exactly conserved. These particles actually receive $O(m_{\text{eff}})$ kicks to their momentum and energy due to the soft interactions with the other N particles participating in the near-collinear $1+N \leftrightarrow 2+N$ process. As mentioned earlier, this leads to a separation in the directions of the splitting particles by angles of order $m_{\text{eff}}/p_{\text{primary}}$. Treating this process as a strictly collinear $1 \leftrightarrow 2$ body process, and neglecting the soft $O(m_{\text{eff}})$ momentum transfers to other particles in the system, is an acceptable approximation because of our assumption that distribution functions (and observables) are smooth functions of momenta. If this assumption were not satisfied, then we could not factorize the collision term into a product of distribution functions and an effective transition rate, as done above. Given our assumed separation of scales, the relative error introduced by this idealization is at most $O(g^\alpha)$, and hence irrelevant in a leading-order treatment. The differential rates γ_{bc}^a are to be understood as summed over spins and colors of all three participants. Their explicit form will be discussed in section V.

III. $2 \leftrightarrow 2$ PARTICLE MATRIX ELEMENTS

Tree-level diagrams for all $2 \leftrightarrow 2$ particle processes in a QCD-like theory are shown in Figure 5. Evaluating these diagrams in vacuum (*i.e.*, neglecting medium-dependent self-energy corrections), squaring the resulting amplitudes, and summing over spins and colors yields the matrix elements shown in Table II.¹⁶ Of course, vacuum matrix elements do not correctly describe the scattering of quasiparticles propagating through a medium. In principle, one should recalculate the diagrams of Fig. 5 including appropriate medium-dependent self-energy and vertex corrections. But with generic hard momenta, for which all Mandelstam variables are of comparable size, these corrections are $O(g^{2\alpha})$ effects and hence ignorable in a leading-order treatment.¹⁷ Medium-dependent effects can give $O(1)$ corrections to matrix elements if any Mandelstam variable is $O(m_{\text{eff}}^2)$. Such momentum regions are phase space suppressed by at least $g^{2\alpha}$ relative to generic hard momenta. Consequently, momentum regions where $s \sim -t \sim -u \sim m_{\text{eff}}^2$ (corresponding to either soft or collinear incoming parti-

¹⁶ Entries in Table II agree with well known QED results and the SU(3) results of Combridge *et. al.* [14].

¹⁷ Spacetime dependence of distribution functions will not be indicated explicitly, but it is important to keep in mind our basic assumption that, in the vicinity of any point x , distributions have negligible spacetime variation on a scale of t_{form} . All results in this and later sections are local; they apply within a region of size t_{form} about any particular point x of interest, using distribution functions evaluated at the point x .

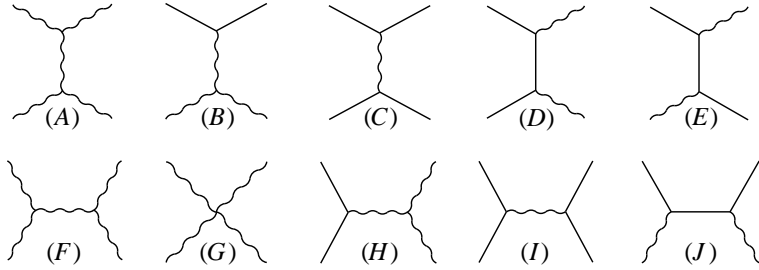


FIG. 5: Lowest-order diagrams for all $2 \leftrightarrow 2$ particle scattering processes in a gauge theory with fermions. Solid lines denote fermions and wiggly lines are gauge bosons. Time may be regarded as running horizontally, either way, so a diagram such as (D) represents both $q\bar{q} \rightarrow gg$ and $gg \rightarrow q\bar{q}$.

$ab \leftrightarrow cd$	$ \mathcal{M}_{cd}^{ab} ^2 / g^4$
$q_1 q_2 \leftrightarrow q_1 q_2$, $q_1 \bar{q}_2 \leftrightarrow q_1 \bar{q}_2$, $\bar{q}_1 q_2 \leftrightarrow \bar{q}_1 q_2$, $\bar{q}_1 \bar{q}_2 \leftrightarrow \bar{q}_1 \bar{q}_2$	$8 \frac{d_F^2 C_F^2}{d_A} \left(\frac{s^2 + u^2}{\underline{t}^2} \right)$
$q_1 q_1 \leftrightarrow q_1 q_1$, $\bar{q}_1 \bar{q}_1 \leftrightarrow \bar{q}_1 \bar{q}_1$	$8 \frac{d_F^2 C_F^2}{d_A} \left(\frac{s^2 + u^2}{\underline{t}^2} + \frac{s^2 + t^2}{\underline{u}^2} \right) + 16 d_F C_F \left(C_F - \frac{C_A}{2} \right) \frac{s^2}{tu}$
$q_1 \bar{q}_1 \leftrightarrow q_1 \bar{q}_1$	$8 \frac{d_F^2 C_F^2}{d_A} \left(\frac{s^2 + u^2}{\underline{t}^2} + \frac{t^2 + u^2}{s^2} \right) + 16 d_F C_F \left(C_F - \frac{C_A}{2} \right) \frac{u^2}{st}$
$q_1 \bar{q}_1 \leftrightarrow q_2 \bar{q}_2$	$8 \frac{d_F^2 C_F^2}{d_A} \left(\frac{t^2 + u^2}{s^2} \right)$
$q_1 \bar{q}_1 \leftrightarrow gg$	$8 d_F C_F^2 \left(\frac{u}{\underline{t}} + \frac{t}{\underline{u}} \right) - 8 d_F C_F C_A \left(\frac{t^2 + u^2}{s^2} \right)$
$q_1 g \leftrightarrow q_1 g$, $\bar{q}_1 g \leftrightarrow \bar{q}_1 g$	$-8 d_F C_F^2 \left(\frac{u}{s} + \frac{s}{\underline{u}} \right) + 8 d_F C_F C_A \left(\frac{s^2 + u^2}{\underline{t}^2} \right)$
$gg \leftrightarrow gg$	$16 d_A C_A^2 \left(3 - \frac{su}{\underline{t}^2} - \frac{st}{\underline{u}^2} - \frac{tu}{s^2} \right)$

TABLE II: Squares of vacuum matrix elements for $2 \leftrightarrow 2$ particle processes in a QCD-like theory, summed over spins and colors of all four particles. Here q_1 and q_2 represent quarks of distinct flavors, \bar{q}_1 and \bar{q}_2 are the associated antiquarks, and g represents a gauge boson. d_F and d_A denote the dimensions of the fundamental and adjoint representations, respectively, while C_F and C_A are the corresponding quadratic Casimirs. In an $SU(N)$ theory with fundamental representation fermions, $d_F = C_A = N$, $C_F = (N^2 - 1)/(2N)$, and $d_A = N^2 - 1$. For a $U(1)$ theory, $d_F = d_A = C_F = 1$ and $C_A = 0$. For $SU(2)$, $d_F = C_A = 2$, $C_F = 3/4$, and $d_A = 3$, while for $SU(3)$, $d_F = C_A = 3$, $C_F = 4/3$, and $d_A = 8$. Terms with underlined denominators are sufficiently infrared sensitive that medium-dependent self-energy corrections must be included, as discussed in the text.

cles) give parametrically suppressed contributions, and medium-dependent corrections can be ignored in these regions. This implies that medium-dependent corrections do not have to be included in terms with denominators of s^2 .¹⁸

More problematic are the regions where $-t$ or $-u$ are $O(m_{\text{eff}}^2)$ while s is large, corresponding to a small angle scattering between hard particles. In this case, some of the matrix elements in the table are enhanced by $O(s/m_{\text{eff}}^2)$ or $O(s^2/m_{\text{eff}}^4)$. In Table II, terms with singly-underlined denominators indicate such infrared-sensitive contributions arising from soft gluon exchange, while terms with double-underlined denominators indicate IR sensitive contributions from a soft exchanged fermion. It is these underlined terms in which medium-dependent effects must be incorporated.¹⁹

For the soft gluon exchange terms one must, in effect, reevaluate the small t (or small u) region of diagrams (A), (B), or (C) with the free gluon propagator on the internal line replaced by the appropriate non-equilibrium retarded gluon propagator,

$$G_{\mu\nu}^{(0)}(Q) = \frac{g_{\mu\nu}}{Q^2} \longrightarrow G_{\mu\nu}^{\text{Ret}}(Q) \equiv [Q^2 + \Pi_{\text{Ret}}(Q)]_{\mu\nu}^{-1}. \quad (3.1)$$

(We have chosen Feynman gauge for convenience, but this is not required.) The required retarded gluon self-energy $\Pi_{\text{Ret}}^{\mu\nu}(Q)$ is discussed in the next section. Evaluating the propagator (3.1) requires, in general, a non-trivial matrix inversion. (The matrix inversion may be performed explicitly in the special case of isotropic distributions; see Appendix A.)

Because the self-energy only matters when the exchange momentum Q is soft, one has considerable freedom in precisely how the substitution (3.1) is implemented. Different choices, all equally acceptable for a leading-order treatment, include the following:

1. Fully reevaluate the gluon exchange diagrams (A), (B), and (C), using the non-equilibrium propagator (3.1) for the internal gluon line.
2. Introduce a separation scale μ satisfying $m_{\text{eff}} \ll \mu \ll p_{\text{hard}}$, and replace the free gluon propagator by the corrected propagator (3.1) only when $Q^2 < \mu^2$.
3. Exploit the fact that soft gluon exchange between hard particles is spin-independent (to leading order) [8]. Write the IR sensitive matrix elements as the result one would have with fictitious scalar quarks, plus an IR insensitive remainder. Replace the IR sensitive part by the correct result for scalar quarks with medium corrections included.

¹⁸ If one were to include self-energy corrections in these s -channel contributions, then there is a potential subtlety if these terms can go on-shell. This is discussed in section VIA, but the conclusion that medium-dependent corrections can be ignored in s -channel processes (when external particles are treated as massless) is unchanged.

¹⁹ Sharp-eyed readers will notice that the $s^2/(tu)$ and $u^2/(st)$ terms appearing in the $qq \leftrightarrow qq$ and $q\bar{q} \leftrightarrow q\bar{q}$ matrix elements (squared) are not underlined, despite the fact that these contributions are infrared-sensitive, albeit less so than the $1/t^2$ or $1/u^2$ terms. The $s^2/(tu)$ and $u^2/(st)$ terms arise from interference between t channel and either u or s channel gluon exchanges. They are sufficiently infrared singular to generate logarithmically divergent rates in the individual gain and loss parts of the collision term, but this log divergence (which would be cutoff by medium effects) cancels when the gain and loss rates are combined. Hence, the apparent IR sensitivity of these terms may be ignored.

The final choice is technically the most convenient. It simply amounts to writing

$$(s^2+u^2)/t^2 = \frac{1}{2} + \frac{1}{2}(s-u)^2/t^2, \quad su/t^2 = \frac{1}{4} - \frac{1}{4}(s-u)^2/t^2, \quad (3.2)$$

and then replacing

$$\frac{(s-u)^2}{t^2} \longrightarrow |G^{\text{Ret}}(P-P')_{\mu\nu}(P+P')^\mu(K+K')^\nu|^2. \quad (3.3)$$

To understand this, note that the square of the vacuum amplitude for t -channel gluon exchange between massless scalars is

$$|G^{(0)}(P-P')_{\mu\nu}(P+P')^\mu(K+K')^\nu|^2 = \left| \frac{(P+P') \cdot (K+K')}{(P-P')^2} \right|^2 = \frac{(s-u)^2}{t^2}. \quad (3.4)$$

For the $1/u^2$ terms, apply the same procedure with $P' \leftrightarrow K'$, which interchanges t and u .

For the soft fermion exchange terms, one must similarly reevaluate the small t (or u) region of diagrams (D) and (E) with the internal free fermion propagator replaced by the non-equilibrium retarded fermion propagator,

$$\frac{1}{Q} = \frac{\mathcal{Q}}{Q^2} \longrightarrow [\mathcal{Q} - \Sigma_{\text{Ret}}(Q)]^{-1} = \frac{\mathcal{Q}}{Q^2}, \quad (3.5)$$

where $\mathcal{Q}^\mu \equiv Q^\mu - \Sigma_{\text{Ret}}^\mu(Q)$. The retarded fermion self-energy $\Sigma_{\text{Ret}}(Q) = \gamma_\mu \Sigma_{\text{Ret}}^\mu(Q)$ is discussed in the next section. In the $q\bar{q} \leftrightarrow gg$ matrix element, the net effect is to replace

$$\frac{u}{t} \longrightarrow \frac{4 \text{Re}[(P \cdot \mathcal{Q})(K \cdot \mathcal{Q})^*] + s \mathcal{Q} \cdot \mathcal{Q}^*}{|\mathcal{Q} \cdot \mathcal{Q}|^2} \quad (3.6)$$

with $\mathcal{Q}^\mu = P^\mu - P'^\mu - \Sigma_{\text{Ret}}^\mu(P-P')$, along with the corresponding replacement with $P' \leftrightarrow K'$ for the tu/u^2 term. For the $qg \leftrightarrow qg$ matrix element, the analogous replacement is

$$\frac{s}{u} \longrightarrow \frac{-4 \text{Re}[(P \cdot \mathcal{Q})(P' \cdot \mathcal{Q})^*] + t \mathcal{Q} \cdot \mathcal{Q}^*}{|\mathcal{Q} \cdot \mathcal{Q}|^2} \quad (3.7)$$

with \mathcal{Q}^μ now equaling $P^\mu - K'^\mu - \Sigma_{\text{Ret}}^\mu(P-K')$. Note that, in general, $|\mathcal{Q} \cdot \mathcal{Q}|^2 \neq (\mathcal{Q} \cdot \mathcal{Q}^*)^2$.

IV. SOFT SCREENING AND HARD EFFECTIVE MASSES

To describe correctly the screening effects which cut off long range Coulomb interactions, we need the non-equilibrium generalization of the standard hard thermal loop (HTL) result for the retarded gauge boson self-energy $\Pi_{\text{Ret}}^{\mu\nu}(Q)$ with soft momentum, $Q = O(m_{\text{eff}})$. The general result for the non-equilibrium case has been previously derived by Mrówczyński and Thoma [15], who obtain²⁰

$$\Pi_{\text{Ret}}^{\mu\nu}(Q) = \sum_s 2\nu_s \frac{g^2 C_s}{d_A} \int \frac{d^3 \mathbf{p}}{2|\mathbf{p}|(2\pi)^3} \frac{\partial f_s(\mathbf{p})}{\partial P^\lambda} \left[-P^\mu g^{\lambda\nu} + \frac{Q^\lambda P^\mu P^\nu}{P \cdot Q - i\varepsilon} \right] \Big|_{P^0=|\mathbf{p}|}, \quad (4.1)$$

²⁰ The normalization of our distribution functions differ from Ref. [15] by a factor of 2, which appears in our expression as the spin degeneracy included in the factor ν_s . To apply (4.1) for momenta Q of order m_{eff} , there is an implicit requirement that the background distributions $f(\mathbf{x}, \mathbf{p}, t)$ not vary significantly on time or distance scales of order $1/m_{\text{eff}}$. This is implied by our basic assumption in this paper that distributions are smooth on the still longer scale of t_{form} .

where ε is a positive infinitesimal.²¹ In this expression, the derivative $\partial f(\mathbf{p})/\partial P^0$ should be understood as zero. The sum runs over all species of excitations (*i.e.*, g , u , \bar{u} , d , \bar{d} , ...), d_A is the dimension of the adjoint representation, and C_s denotes the quadratic Casimir in the color representation appropriate for species s .²² (See the caption of Table II for specializations.) The self-energy (4.1) can also be rewritten in the form²³

$$\Pi_{\text{Ret}}^{\mu\nu}(Q) = \sum_s 2\nu_s \frac{g^2 C_s}{d_A} \int \frac{d^3\mathbf{p}}{2|\mathbf{p}|(2\pi)^3} f_s(\mathbf{p}) \left[g^{\mu\nu} - Q \cdot \partial_P \frac{P^\mu P^\nu}{P \cdot Q - i\varepsilon} \right] \Big|_{P^0=|\mathbf{p}|}, \quad (4.2)$$

which is manifestly symmetric in the indices μ and ν . Simpler expressions may be given in the special case of isotropic distributions [16], where $\Pi_{\text{Ret}}(Q)$ has the same form as the equilibrium HTL result, but with a value of the Debye mass proportional to the integral \mathcal{J} [Eq. (1.6)] over the distribution $f(|\mathbf{p}|)$. This is summarized in Appendix A.

We mention in passing that the result (4.1) for $\Pi_{\text{Ret}}(Q)$ makes the implicit assumption that distributions $f(\mathbf{p})$ do not vary significantly for changes of momentum of order \mathbf{q} [which is $O(m_{\text{eff}})$ in the case of interest]. Specifically, the derivation of (4.1) assumes that $f(\mathbf{p}+\mathbf{q}) - f(\mathbf{p})$ can be approximated as $\mathbf{q} \cdot \nabla_{\mathbf{p}} f(\mathbf{p})$.

We also need the corresponding self-energy $\Sigma_{\text{Ret}}(Q)$ for fermions with soft momentum Q , because this cuts off the small momentum-transfer behavior of fermion exchange diagrams like Fig. 2. This was also derived by Mrówczyński and Thoma [15] but their result has a factor of 4 error. The corrected expression for a fermion of flavor s is $\Sigma_{\text{Ret},s}(Q) = \gamma_\mu \Sigma_{\text{Ret},s}^\mu(Q)$ with

$$\Sigma_{\text{Ret},s}^\mu(Q) = -g^2 C_F \int \frac{d^3\mathbf{p}}{2|\mathbf{p}|(2\pi)^3} [2f_g(\mathbf{p}) + f_s(\mathbf{p}) + f_{\bar{s}}(\mathbf{p})] \frac{P^\mu}{P \cdot Q - i\varepsilon} \Big|_{P^0=|\mathbf{p}|}, \quad (4.3)$$

where f_g , f_s , and $f_{\bar{s}}$ are the gluon, fermion, and anti-fermion distributions respectively (as always, per helicity and color state). The simple gamma-matrix structure $\not{\Sigma}$ is a consequence of the chiral symmetry which results from the neglect of zero temperature fermion masses (relative to their medium-dependent effective mass).

In addition to these soft self-energies, we will also need medium-dependent corrections to dispersion relations for hard particles that are nearly on-shell. These will enter in the formulas that determine the near-collinear “ $1 \leftrightarrow 2$ ” rates. As noted in the introduction, the resulting dispersion relation corrections for hard excitations, at leading order, turn out to take the simple form

$$Q^2 + m_{\text{eff}}^2 = 0. \quad (4.4)$$

with a medium-dependent mass m_{eff} . An efficient way to derive the values of these masses is by using the previous results for soft self-energies, which are valid for $Q \ll p_{\text{screen}}$, in the

²¹ We use a $(-+++)$ metric.

²² For Abelian theories, replace $g^2 C_s$ by the charge (squared) of the corresponding particle.

²³ To obtain this, replace $d^3\mathbf{p}/2|\mathbf{p}|$ in expression (4.1) by $d^4P \delta(P^2) \Theta(P^0)$. Then integrate by parts, noting that the contribution where the derivative hits the delta function generates a factor of P^λ , which vanishes when combined with the bracketed expression in (4.1). Then perform the P^0 integral to get back to $d^3\mathbf{p}$.

intermediate regime $m_{\text{eff}} \ll Q \ll p_{\text{screen}}$, where both the HTL approximation and the hard dispersion relation (4.4) are valid.²⁴

Consider hard gauge bosons first. Only transverse polarizations are relevant because the longitudinal polarization decouples for hard momenta. We can use the massless dispersion relation $Q^2 = 0$ when evaluating the self-energy (4.2) for the purpose of obtaining the first correction to the dispersion relation. Working in light-cone coordinates defined by the direction of \mathbf{q} , the second term in brackets in (4.2) is then proportional to

$$Q^+ \frac{\partial}{\partial P^+} \left(\frac{P^\mu P^\nu}{P^- Q^+ - i\varepsilon} \right). \quad (4.5)$$

For transverse choices of μ and ν , the derivative vanishes. So the effective mass $m_{\text{eff,g}}$ of hard (transverse) gauge bosons comes only from the first term of (4.2), giving

$$m_{\text{eff,g}}^2 = \sum_s 2\nu_s \frac{g^2 C_s}{d_A} \int \frac{d^3 \mathbf{p}}{2|\mathbf{p}|(2\pi)^3} f_s(\mathbf{p}). \quad (4.6)$$

Now consider hard fermions. The effective Dirac equation is

$$[\mathcal{Q} - \Sigma_{\text{Ret}}(Q)] \psi = 0. \quad (4.7)$$

Multiplying on the left by another factor of $(\mathcal{Q} - \Sigma_{\text{Ret}})$ gives the condition

$$(Q - \Sigma_{\text{Ret}})^2 = Q^2 - 2Q \cdot \Sigma_{\text{Ret}} + \Sigma_{\text{Ret}}^2 = 0, \quad (4.8)$$

so that, to leading non-trivial order, the on-shell dispersion relation for hard fermions is

$$Q^2 = 2Q \cdot \Sigma_{\text{Ret}}(Q). \quad (4.9)$$

From the result (4.3) for the self-energy, we immediately find that the effective mass for a hard fermion of flavor s is given by

$$m_{\text{eff},s}^2 = 2g^2 C_F \int \frac{d^3 \mathbf{p}}{2|\mathbf{p}|(2\pi)^3} [2f_g(\mathbf{p}) + f_s(\mathbf{p}) + f_{\bar{s}}(\mathbf{p})]. \quad (4.10)$$

Note that the hard effective masses (4.6) and (4.10) are independent of the direction of the momentum \mathbf{q} of the excitation, as well as its spin, even in the presence of general anisotropic distributions $f(\mathbf{p})$. This is in contrast to soft screening, since the self-energy $\Pi_{\text{Ret}}^{\mu\nu}(Q)$, given by (4.1), generically depends on the direction of \mathbf{q} if distributions are not isotropic. The spin independence and isotropy of these (leading order) effective masses holds provided only that distribution functions are not themselves polarized. [This assumption underlies the HTL results (4.1) and (4.3).] This is special feature of hot gauge theories;

²⁴ Some readers may wonder whether there can be $O(Q/p_{\text{screen}})$ effects in the self-energy that were dropped in the HTL approximation but which affect the hard dispersion relation for $Q \gtrsim p_{\text{screen}}$, and which would cause m_{eff} to be a non-trivial function of Q/p_{screen} instead of a constant. One can check by explicit diagrammatic analysis of self-energies that, for $Q^2 = 0$, this does not happen for fermions, scalars, or transverse gauge bosons.

in a generic anisotropic medium, no symmetry argument prevents splitting of dispersion relations into different branches depending on the spin of an excitation. In other words, a generic anisotropic medium is birefringent.

If the self-energies (4.1) or (4.3) had led to spin-dependent dispersion relations for hard excitations, then even if distributions were not polarized at some initial time, the subsequent evolution of excitations through the birefringent medium would generate spin asymmetries. For such a system, it would be inconsistent to formulate an effective theory with spin independent but anisotropic distribution functions. Fortunately, hot gauge theories do not behave this way.

V. “1 \leftrightarrow 2” PARTICLE PROCESSES

A. Basic formulas

The appropriate splitting/joining rates γ_{bc}^a characterizing near-collinear “1 \leftrightarrow 2” processes may be extracted from Ref. [8]. Let $\hat{\mathbf{n}}$ be a unit vector in the direction of propagation of the splitting (or merging) hard particles, so that $\mathbf{p} = p \hat{\mathbf{n}}$, $\mathbf{p}' = p' \hat{\mathbf{n}}$, and $\mathbf{k} = k \hat{\mathbf{n}}$. Then the required color and spin-summed effective matrix elements, consistently incorporating the LPM effect at leading order, may be expressed as

$$\gamma_{qg}^q(p\hat{\mathbf{n}}; p'\hat{\mathbf{n}}, k\hat{\mathbf{n}}) = \gamma_{q\bar{q}}^{\bar{q}}(p\hat{\mathbf{n}}; p'\hat{\mathbf{n}}, k\hat{\mathbf{n}}) = \frac{p'^2 + p^2}{p'^2 p^2 k^3} \mathcal{F}_q^{\hat{\mathbf{n}}}(p, p', k), \quad (5.1a)$$

$$\gamma_{q\bar{q}}^g(p\hat{\mathbf{n}}; p'\hat{\mathbf{n}}, k\hat{\mathbf{n}}) = \frac{k^2 + p'^2}{k^2 p'^2 p^3} \mathcal{F}_q^{\hat{\mathbf{n}}}(k, -p', p), \quad (5.1b)$$

$$\gamma_{gg}^g(p\hat{\mathbf{n}}; p'\hat{\mathbf{n}}, k\hat{\mathbf{n}}) = \frac{p'^4 + p^4 + k^4}{p'^3 p^3 k^3} \mathcal{F}_g^{\hat{\mathbf{n}}}(p, p', k), \quad (5.1c)$$

where

$$\mathcal{F}_s^{\hat{\mathbf{n}}}(p', p, k) \equiv \frac{d_s C_s \alpha}{2(2\pi)^3} \int \frac{d^2 h}{(2\pi)^2} 2\mathbf{h} \cdot \text{Re } \mathbf{F}_s^{\hat{\mathbf{n}}}(\mathbf{h}; p', p, k) \quad (5.2)$$

and $\alpha \equiv g^2/(4\pi)$. The function $\mathbf{F}_s^{\hat{\mathbf{n}}}(\mathbf{h}; p', p, k)$, for fixed given values of p' , p , k and $\hat{\mathbf{n}}$, depends on a two-dimensional vector \mathbf{h} which is perpendicular to $\hat{\mathbf{n}}$. $\mathbf{F}_s^{\hat{\mathbf{n}}}$ is the solution to the linear integral equation

$$\begin{aligned} 2\mathbf{h} = i \delta E(\mathbf{h}; p', p, k) \mathbf{F}_s^{\hat{\mathbf{n}}}(\mathbf{h}; p', p, k) + g^2 \int \frac{d^4 Q}{(2\pi)^4} 2\pi \delta(v_{\hat{\mathbf{n}}} \cdot Q) v_{\hat{\mathbf{n}}}^\mu v_{\hat{\mathbf{n}}}^\nu \langle\langle A_\mu(Q) [A_\nu(Q)]^* \rangle\rangle \\ \times \left\{ (C_s - \frac{1}{2} C_A) [\mathbf{F}_s^{\hat{\mathbf{n}}}(\mathbf{h}; p', p, k) - \mathbf{F}_s^{\hat{\mathbf{n}}}(\mathbf{h} - k \mathbf{q}_\perp; p', p, k)] \right. \\ \left. + \frac{1}{2} C_A [\mathbf{F}_s^{\hat{\mathbf{n}}}(\mathbf{h}; p', p, k) - \mathbf{F}_s^{\hat{\mathbf{n}}}(\mathbf{h} + p' \mathbf{q}_\perp; p', p, k)] \right. \\ \left. + \frac{1}{2} C_A [\mathbf{F}_s^{\hat{\mathbf{n}}}(\mathbf{h}; p', p, k) - \mathbf{F}_s^{\hat{\mathbf{n}}}(\mathbf{h} - p \mathbf{q}_\perp; p', p, k)] \right\}, \quad (5.3) \end{aligned}$$

which sums up multiple interactions. The four-vector $v_{\hat{\mathbf{n}}} \equiv (1, \hat{\mathbf{n}})$ is a null vector in the direction of $\hat{\mathbf{n}}$, and the vector \mathbf{q}_\perp is the part of \mathbf{q} perpendicular to $\hat{\mathbf{n}}$. Once again, d_s and

C_s are the dimension and quadratic Casimir of the color representation for species s . The energy difference δE is defined as

$$\delta E(\mathbf{h}; p', p, k) = \frac{m_{\text{eff},g}^2}{2k} + \frac{m_{\text{eff},s}^2}{2p} - \frac{m_{\text{eff},s}^2}{2p'} + \frac{\mathbf{h}^2}{2p k p'} \quad (5.4)$$

and represents the energy denominator $\epsilon_g(\mathbf{k}) + \epsilon_s(\mathbf{p}) - \epsilon_s(\mathbf{p}')$ which appears in a $p' \leftrightarrow pk$ splitting process. The variable \mathbf{h} is related to the transverse momentum; see Ref. [8] for details. We will discuss momentarily the required correlator $\langle\langle A_\mu(Q)[A_\nu(Q)]^* \rangle\rangle$ of the soft gauge field.

Ref. [8], from which the above formulas for γ_{bc}^a were extracted, culminated in the derivation of the near-collinear “1 \leftrightarrow 2” contribution to the total differential gluon production rate $d\Gamma_g/d^3k$ for hard gluons with momentum k . In order to facilitate comparison with that reference, we show in Appendix B how to express the near-collinear contribution to $d\Gamma_g/d^3k$ in terms of the γ_{bc}^a differential rates.

The final element we need is the mean square fluctuations in soft momentum components of the gauge field in the medium, $\langle\langle A_\mu(Q)[A_\nu(Q)]^* \rangle\rangle$. Formally, this is the Fourier transform of the (non-equilibrium) HTL approximation to the Wightman gauge field correlator,²⁵ excluding the momentum and color conservation delta functions,

$$\int d^4x d^4y e^{i(Q' \cdot y - Q \cdot x)} \langle\langle A_\mu^a(x) A_\nu^b(y) \rangle\rangle \equiv (2\pi)^4 \delta^{(4)}(Q - Q') \delta^{ab} \langle\langle A_\mu(Q)[A_\nu(Q)]^* \rangle\rangle. \quad (5.5)$$

This correlator characterizes the stochastic background fluctuations in which collinear splitting processes take place (see Ref. [8]). We are interested in the correlator for space-like 4-momenta Q , and physically (at leading order) it represents the correlation of the screened color fields carried by on-shell hard particles streaming randomly through the plasma. Hence, it may be understood as the (absolute) square of the amplitude shown in Fig. 6 integrated over the phase space of the hard particle, where the gauge propagator is to be understood as including the medium-dependent self-energy. This leads to

$$\langle\langle A_\mu(Q)[A_\nu(Q)]^* \rangle\rangle = G_{\mu\alpha}^{\text{Ret}}(Q) \Pi_{12}^{\alpha\beta}(Q) [G_{\nu\beta}^{\text{Ret}}(Q)]^*, \quad (5.6)$$

where $G^{\text{Ret}}(Q)$ is the retarded propagator on the right side of (3.1) and

$$\Pi_{12}^{\alpha\beta}(Q) \equiv \sum_s \nu_s \frac{g^2 C_s}{d_A} \int \frac{d^3\mathbf{k}}{(2\pi)^3} v_\mathbf{k}^\alpha v_\mathbf{k}^\beta f_s(\mathbf{k}) [1 \pm f_s(\mathbf{k} + \mathbf{q})] 2\pi \delta(E_{\mathbf{k}+\mathbf{q}} - E_\mathbf{k} - q^0) \quad (5.7)$$

for soft momenta Q . Here, $v_\mathbf{k} \equiv (1, \hat{\mathbf{k}})$ is the 4-velocity of a hard particle with momentum \mathbf{k} and $g v_\mathbf{k}$ gives the current of this particle up to group factors. The f 's appear as initial state

²⁵ Not to be confused with time-ordered or retarded correlators of the gauge field. Once again, our basic assumption is that distribution functions are smooth on a time and distance scale of t_{form} associated with the duration of a near-collinear “1 \leftrightarrow 2” process. Hence, for the purpose of evaluating the non-equilibrium correlator in (5.5) for momenta of order m_{eff} , distribution functions may be treated as x -independent. Spacetime variation in the non-equilibrium state will, of course, smear out the momentum conserving delta function in (5.5), but only by an amount which is irrelevant for our leading order treatment.

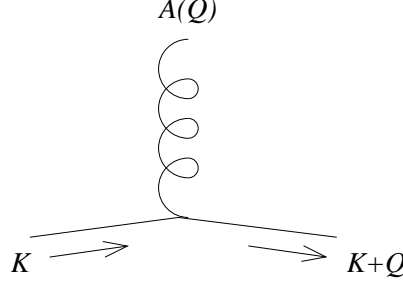


FIG. 6: Amplitude for the gauge field created by an on-shell hard particle in the medium.

distributions and final-state Bose enhancement or Fermi blocking factors. For soft momenta Q , expression (5.7) may be simplified to give

$$\Pi_{12}^{\alpha\beta}(Q) = \sum_s \nu_s \frac{g^2 C_s}{d_A} \int \frac{d^3 \mathbf{k}}{(2\pi)^3} v_{\mathbf{k}}^{\alpha} v_{\mathbf{k}}^{\beta} f_s(\mathbf{k}) [1 \pm f_s(\mathbf{k})] 2\pi \delta(v_{\mathbf{k}} \cdot Q). \quad (5.8)$$

One may alternatively derive this by summing hard thermal loops into the propagator of the Schwinger-Keldysh formalism, one of whose components gives the Wightman correlator.²⁶ This is the origin of our notation Π_{12} above, which is the one-loop Wightman current-current correlator and is an off-diagonal component of the self-energy in this formalism.

In the special case of isotropic distribution functions, one can simplify substantially the expression (5.8) for $\Pi_{12}(Q)$. Moreover, one can analytically reduce the $d^4 Q$ integral appearing in the integral equation (5.3) to a two-dimensional integral over \mathbf{q}_\perp . See Appendix A for details.

In equilibrium, the Wightman correlator is related to the retarded correlator by the fluctuation-dissipation theorem, which gives

$$\begin{aligned} \langle\langle A_\mu(Q) [A_\nu(Q)]^* \rangle\rangle_{\text{equilibrium}} &= 2[n(q^0) + 1] \text{Im } G_{\mu\nu}^{\text{Ret}}(Q) \\ &= -2[n(q^0) + 1] G_{\mu\alpha}^{\text{Ret}}(Q) [\text{Im } \Pi_{\text{Ret}}^{\alpha\beta}(Q)] [G_{\nu\beta}^{\text{Ret}}(Q)]^*, \end{aligned} \quad (5.9)$$

where $n(\epsilon) = [e^{\beta\epsilon} - 1]^{-1}$ is the usual equilibrium Bose distribution. For soft Q , the prefactor $2[n(q^0) + 1]$ can be replaced by $2T/q^0$. It is instructive to compare the non-equilibrium formula (5.8) for $\Pi_{12}(Q)$ with that for $\text{Im } \Pi_{\text{Ret}}(Q)$. The latter, for soft Q , can be extracted from the earlier expression (4.1) which gives

$$\text{Im } \Pi_{\text{Ret}}^{\alpha\beta}(Q) = \sum_s \nu_s \frac{g^2 C_s}{d_A} \int \frac{d^3 \mathbf{k}}{(2\pi)^3} v_{\mathbf{k}}^{\alpha} v_{\mathbf{k}}^{\beta} [\mathbf{q} \cdot \nabla_{\mathbf{k}} f_s(\mathbf{k})] \pi \delta(v_{\mathbf{k}} \cdot Q). \quad (5.10)$$

The fluctuation-dissipation theorem (5.9) is satisfied in equilibrium by the results (5.8) and (5.10) for soft Q because equilibrium Bose or Fermi distribution functions $n_s(\epsilon) = [e^{\beta\epsilon} \mp 1]^{-1}$ satisfy

$$\mathbf{q} \cdot \nabla_{\mathbf{k}} n(\epsilon) = -\beta \mathbf{v} \cdot \mathbf{q} n_s(\epsilon) [1 \pm n_s(\epsilon)]. \quad (5.11)$$

²⁶ For a general introduction, see chapter X of Ref. [17]. See also, for example, Eqs. (A34) and (A23) of Ref. [18].

B. The formation time

Earlier, we promised an explanation of the parametric formulas (1.10) and (1.11) for the formation time t_{form} of a near-collinear “1 \leftrightarrow 2” process and for the number N_{form} of soft collisions that take place in that time. We will give here a brief, superficial review, using the notation we have adopted in this paper. For a more thorough discussion of the scales set by the LPM effect, the reader should consult the literature, such as Refs. [19–21]. We could deduce the scales by discussing the qualitative behavior of solutions of the actual equations (5.2) and (5.3) which incorporate the required physics, much as we did in the context of photo-emission in Ref. [11]. Instead, however, we will give here a more physical discussion which leads to the same results.

One way to understand the basic scales is to begin by considering classical (soft) bremsstrahlung radiation of photons (rather than gluons), with wave number k_γ , emitted by a classical charged particle moving very close to the speed of light that undergoes N random small-angle collisions. (This was the original classical picture of Landau and Pomeranchuk [22].) Let τ be the mean time between those collisions and θ_1 the typical angle of deflection from each collision. The total deflection is then $\theta \sim \sqrt{N} \theta_1$, which we shall assume is small. If τ is very large, there will on average be no interference between the bremsstrahlung fields created by successive collisions (for fixed k_γ). If τ is very small, the bremsstrahlung field will not be able to resolve the individual collisions, and the field will be the same as that from a single collision by the total angle θ . Since bremsstrahlung is at most logarithmically sensitive to the scattering angle θ , this smearing of N collisions into one collision will reduce the power radiated at this wavenumber by a factor of roughly N compared to what it would be if each collision could be treated independently. That is the LPM effect.

The classical bremsstrahlung field from a scattering by angle θ is dominated by radiation inside a cone of angle roughly θ . The first and last scatterings, at space-time points x_1 and x_N , will interfere significantly together if the phases in the factors $\exp(K_\gamma \cdot x_1)$ and $\exp(K_\gamma \cdot x_2)$ are comparable. For random collisions, that will happen if $K_\gamma \cdot (x_N - x_1) \ll 1$, which, for small θ , gives²⁷

$$k_\gamma N \tau (1 - \cos \theta) \sim k_\gamma N \tau \theta^2 \ll 1. \quad (5.12)$$

We have taken $x_N^0 - x_1^0 \simeq |\mathbf{x}_N - \mathbf{x}_1| \sim N \tau$ since the particle moves on nearly a straight-line trajectory at the speed of light. For $k_\gamma N \tau \theta^2 \gg 1$, in contrast, the bremsstrahlung produced by the first and last collisions will be independent. The crossover criterion $k_\gamma N \tau \theta^2 \sim 1$, with $\theta^2 \sim N \theta_1^2$, then determines the typical number of collisions which are effectively smeared together by the LPM effect:

$$N \sim 1 / \sqrt{k_\gamma \tau \theta_1^2}, \quad (5.13)$$

except that N must always be at least 1, since there must be a scattering to produce classical bremsstrahlung.

²⁷ For sharp single collisions ($N=1$), there are actually two angular scales: the deflection angle θ of the charged particle and the angle θ_γ that \mathbf{k}_γ makes with the initial or final directions of the particle (whichever is smaller). There can then be logarithms arising from considering $\theta_\gamma \ll \theta$ in the bremsstrahlung rate, which we ignore.

A classical treatment of radiation breaks down when k_γ is no longer small compared to the energy E of the radiating charged particle. However, parametric estimates (as opposed to precise classical formulas) are still valid where the classical treatment first begins to break down. So we can still use the estimate (5.13) for N when $k_\gamma \sim E$, provided $E - k_\gamma$ is not parametrically small compared to E . In a single soft collision of a hard particle with energy E , the typical deflection angle is

$$\theta_1 \sim \frac{q_\perp}{E}, \quad (5.14)$$

where q_\perp is the typical transverse momentum transfer. Inserting this into (5.13) and setting $k_\gamma \sim E$ gives

$$N \sim \max \left(1, \sqrt{E/(\tau q_\perp^2)} \right). \quad (5.15)$$

This estimate for hard bremsstrahlung applies equally well to the case of gluon emission. Setting $q_\perp \sim m_{\text{eff}}$ gives the estimate (1.11) previously quoted for N_{form} .

When the formation time is large compared to τ , then it is simply $N\tau$ by the definitions of N and τ . But if $\tau \gg E/q_\perp^2$, so that emission from different soft collisions do not significantly interfere, then the formation time is the time scale t_1 associated with bremsstrahlung from a single isolated collision. Classically, this is the time Δx^0 for which $K_\gamma \cdot \Delta x \sim 1$, which gives $k_\gamma t_1 \theta_1^2 \sim 1$ and

$$t_1 \sim \frac{1}{k_\gamma \theta_1^2} \sim \frac{E^2}{k_\gamma q_\perp^2} \sim \frac{E}{q_\perp^2}, \quad (5.16)$$

for $k_\gamma \sim E$. This same result can be found by examining how far off-shell in energy the internal hard line is in the basic bremsstrahlung processes of Fig. 3. One can nicely combine both cases in the single formula

$$t_{\text{form}} \sim \frac{E}{N q_\perp^2}, \quad (5.17)$$

which, upon taking $q_\perp \sim m_{\text{eff}}$, gives the earlier quoted result (1.10).²⁸

We specialized to $k_\gamma \sim E$ above. In this regime, the above estimates are equally applicable to photon or gluon emission. The behavior of the formation time for $k_\gamma \ll E$ is not critical to understanding the conditions for applying our effective theory to the evolution of hard primaries. The dominant energy loss mechanism for primaries is via hard gluon emission processes with $k_g \sim E$ rather than $k_g \ll E$ soft emissions. However, it is interesting to note that for soft emission, the case of photon emission is qualitatively different from gluon emission. Eqs. (5.13) and (5.16) show that the formation time for photons is much longer

²⁸ Replacing q_\perp by m_{eff} in the estimates (5.15) and (5.17) amounts to an implicit assumption that the only important collisions are soft collisions with momentum transfers of order m_{eff} . Harder collisions are rarer than soft collisions. However, as noted in footnote 5, a single collision by an angle $\theta \sim \sqrt{N} m_{\text{eff}}/E$ is no rarer than N consecutive soft collisions, each by angle m_{eff}/E . For large N , the same could be said of, for example, $N/10$ consecutive collisions, each by angle $\sqrt{10} m_{\text{eff}}/E$. This multiplicity of possibilities turns out to result in logarithmic corrections to the above analysis. Throughout this paper, we have consistently ignored logarithms in parametric estimates, and we continue to do so here. We have also ignored the effect of effective thermal masses, which cause hard particles to move slightly slower than the speed of light. For $q_\perp \gtrsim m_{\text{eff}}$, however, this does not affect any of our parametric estimates.

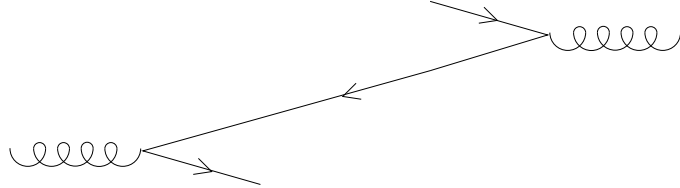


FIG. 7: The t -channel diagram for $qg \rightarrow qg$, drawn as a time-ordered diagram with time running from left to right.

for $k_\gamma \ll E$ than it is for $k_\gamma \sim E$. This is not true for gluon emission. Because the gluon can scatter by strong interactions, it cannot maintain its coherence over as long a time scale as a photon can. Soft scatterings involving the emitted gluon can change its direction by angles of order $q_\perp/k_g \sim m_{\text{eff}}/k_g$, which increase as k_g decreases. Consequently, gluon bremsstrahlung with $k_g \ll E$ is actually less coherent than gluon bremsstrahlung with k_g of order $E/2$. For gluon emission where the LPM effect is significant, the longest formation time is for the case where the energies of the two final particles are comparable.

VI. DISCUSSION

A. Dispersion relation corrections and double counting

In section III we asserted that medium-dependent dispersion relation corrections on external lines are, for hard particles, sub-leading corrections which may be neglected. There is, however, a potential subtlety concerning whether or not the internal line in a $2 \leftrightarrow 2$ process is kinematically allowed to go on-shell. If this occurs, then the $2 \leftrightarrow 2$ particle collision rate will include the contribution from an on-shell $2 \rightarrow 1$ process followed by a subsequent $1 \rightarrow 2$ process. Given the presence of explicit $1 \leftrightarrow 2$ particle collision terms in our effective theory, this would be inappropriate double-counting of the underlying scattering events.

Consider, for example, the t -channel $qg \rightarrow qg$ process illustrated in Fig. 7. To incorporate a correct treatment of small angle scattering, as discussed in section III, one must include the HTL fermion self-energy (4.3) on the internal quark line. If medium-dependent effective masses are included on the external lines, then the internal quark line can go on-shell if $m_{\text{eff},g} > 2m_{\text{eff},q}$. This condition is not satisfied in equilibrium QCD, but it can be satisfied with non-equilibrium distributions. It can also be satisfied, in equilibrium, in certain QCD-like theories.²⁹ If this condition is satisfied, then the on-shell pole in the fermion propagator will generate a divergence in the two body collision term $C^{2 \leftrightarrow 2}$. This divergence arises from an integration over the time difference between the creation and destruction of the virtual intermediate fermion, and reflects the fact that a calculation which just includes the HTL self-energy (4.3) is modeling that excitation as having an infinite lifetime.³⁰ This divergence is, of course, unphysical and would effectively be replaced by the transport mean free time

²⁹ For example, equilibrium SU(3) gauge theories with N_f Dirac fermions have $m_{\text{eff},g} = (\frac{1}{2} + \frac{1}{12}N_f)^{1/2} gT$ and $m_{\text{eff},q} = \frac{1}{\sqrt{3}} gT$. Hence $m_{\text{eff},g} > 2m_{\text{eff},q}$ if $N_f > 10$.

³⁰ This is because the HTL self-energies (4.1) and (4.3) have no imaginary part for timelike 4-momenta Q .

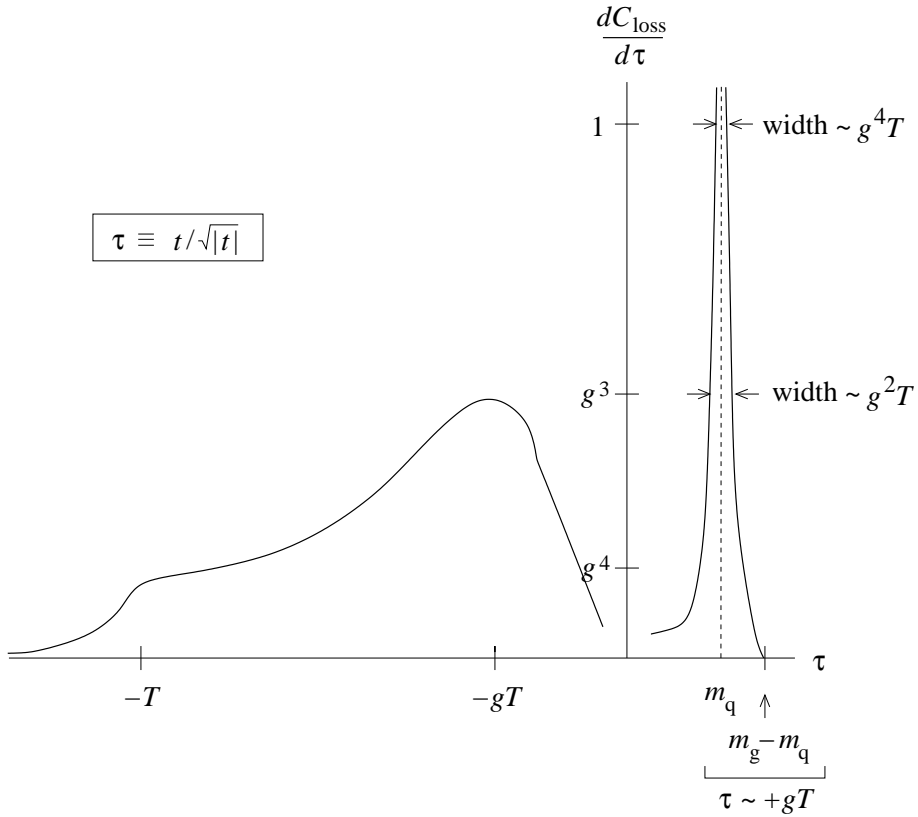


FIG. 8: A qualitative sketch of the purely t -channel contribution of Fig. 7 for $qg \leftrightarrow qg$ to the loss part of the $2 \leftrightarrow 2$ collision term for a hard gluon or quark, plotted as $dC_{\text{loss}}^{2 \leftrightarrow 2} / d\tau$ vs. τ where $\tau \equiv t / \sqrt{|t|}$. Interferences with other channels are ignored. The labels m_q and m_g are short-hand for the hard effective quark and gluon masses $m_{\text{eff},q}$ and $m_{\text{eff},g}$, and we have assumed $m_{\text{eff},g} > 2m_{\text{eff},q}$. The other scales listed above (1, g^4 , T , etc.) only denote parametric orders.

if further interactions with the medium were properly included.³¹

This situation is depicted in more detail (but still qualitatively) in Fig. 8, which shows the contribution to the loss part of the collision term $C^{2 \leftrightarrow 2}$ (for hard particles) from t -channel $qg \leftrightarrow qg$ scattering, as a function of the invariant momentum transfer. For simplicity of presentation, this figure assumes that the momenta of scatterers, screeners and primaries are all within an $O(1)$ factor of a common scale T , and that the phase space distributions of all excitations on these scales are $O(1)$. In other words, the system is at most an $O(1)$ deviation from equilibrium. We have found it convenient to use $\tau \equiv t / \sqrt{|t|}$ rather than t , and have sketched $dC_{\text{loss}}^{2 \leftrightarrow 2} / d\tau$ vs. τ . If the external particles were massless, then t (and hence

³¹ One natural sounding but inadequate solution is to include the full thermal width on the intermediate line. However, this width is logarithmically IR divergent (in perturbation theory) due to sensitivity to long wavelength non-perturbative fluctuations in the gauge field. Moreover, merely including a width without simultaneously including additional interactions with the medium incorporates the wrong physics; the width is dominated by soft scattering, but a soft scattering event does not prevent the on-shell intermediate particle from propagating a large distance before breaking up.

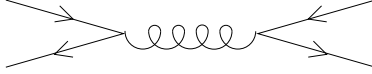


FIG. 9: s -channel diagram for $q\bar{q} \rightarrow q\bar{q}$.

τ) would always be negative. The behavior between $\tau \sim -T$ and $\tau \sim -gT$ is $dC/d\tau \sim g^4/\tau$ and is responsible for a leading-log contribution to the collision term. The (exaggerated) fall-off depicted for $\tau \ll -T$ reflects the decrease of initial state distributions for momenta large compared to T . The fall-off just above $\tau \sim -gT$ is due to screening (that is, due to the inclusion of the HTL self-energy for the internal quark line). For $\tau \lesssim -gT$, the contributions to $C_{\text{loss}}^{2\leftrightarrow 2}$ are dominated by hard initial particles whose trajectories intersect at an angle θ_{12} of order 1. Each particle is deflected in the collision by an angle of order $|\tau|/T$. The contributions in this kinematic region are not sensitive, at leading order, to whether or not one uses massive or massless dispersion relations for the external lines. In contrast, for $\tau > 0$, the contributions are dominated by hard initial particles that are nearly collinear, with $\theta_{12} \sim g$. The peak at $\tau = m_{\text{eff},q}$ represents the nearly-collinear process of Fig. 7. [Kinematics forces this process to be nearly collinear because the $O(gT)$ masses $m_{\text{eff},q}$ and $m_{\text{eff},g}$ are small compared to the hard $O(T)$ momenta.]

From the plot, one can see that two regions make significant contributions to the collision term. The first region is $-T \lesssim \tau \lesssim gT$, which reflects genuine $2 \leftrightarrow 2$ processes and makes an $O(g^4T)$ contribution to C_{loss} . The second region is $|\tau - m_{\text{eff},q}| \lesssim g^4T$, which is double counting and incorrectly treating the $1 \leftrightarrow 2$ processes that are described by the “ $1 \leftrightarrow 2$ ” collision term. Fortunately, our treatment of “ $1 \leftrightarrow 2$ ” processes correctly handles off-shellness in energy as large as the inverse formation time $O(g^2T)$ (see section IA) and so already correctly accounts for the physics in this region where the energy is off-shell by only $\lesssim g^4T$. Note that τ ’s further out on the peak at $m_{\text{eff},q}$ in Fig. 1 (for instance, $|\tau - m_{\text{eff},q}| \sim g^2T$), give a contribution to C_{loss} from this particular diagram that is subleading compared to genuine $2 \leftrightarrow 2$ contributions and which may therefore be ignored.

To formulate a correct collision term which only includes “genuine” $2 \leftrightarrow 2$ processes, one must somehow keep the contribution from the first region and eliminate the second. Although there are many ways one could accomplish this, the simplest solution is to include the HTL self-energy on internal lines (where it is needed to describe screening) but to treat external lines as massless.

Exactly the same issue can arise with s -channel processes, as illustrated in Fig. 9 for $q\bar{q} \leftrightarrow q\bar{q}$. A plot analogous to the one discussed above, but this time showing the contribution to $dC_{\text{loss}}^{2\leftrightarrow 2}/d\sqrt{s}$ vs. \sqrt{s} for this s -channel annihilation reaction, is shown in Fig. 10. If HTL self-energies are included in the internal gluon line, then the virtual gluon can go on-shell in this $q\bar{q} \rightarrow g \rightarrow q\bar{q}$ process even when the external quarks are treated as massless, since two massless particles are kinematically allowed to combine to create one massive one. For s -channel processes, however, it is not necessary to include HTL self-energies on the internal line in the first place. Unlike the case of t and u -channel processes, they are not required to control infrared sensitivity. So one solution which avoids all partial double counting of $1 \leftrightarrow 2$ processes while not affecting the leading-order result for the true $2 \leftrightarrow 2$ contributions is to treat all external particles as massless, and include HTL self-energies in t -channel and

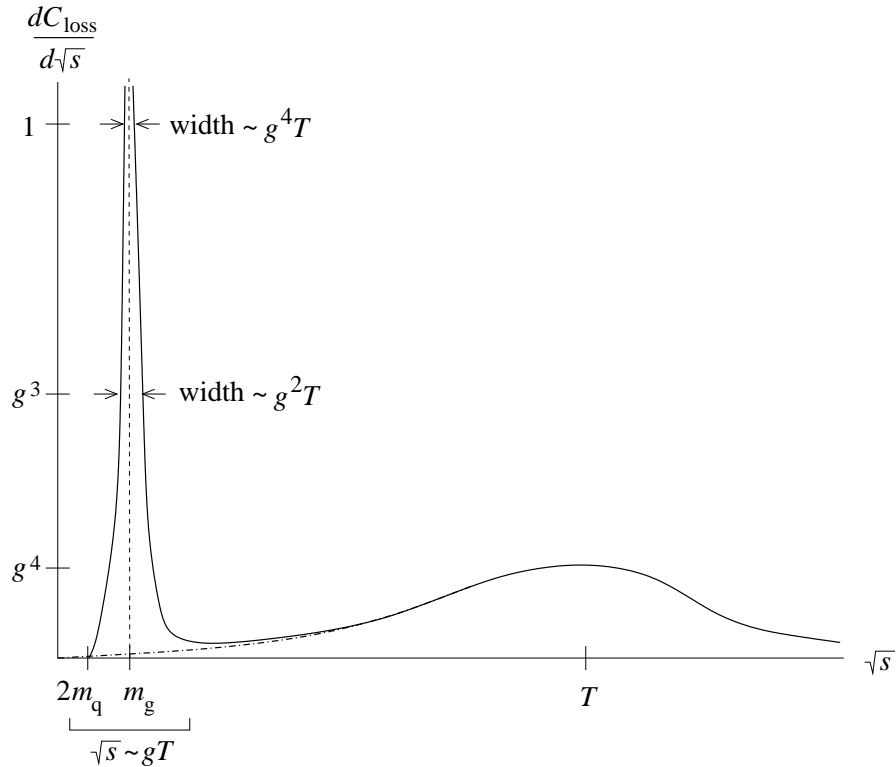


FIG. 10: A qualitative sketch of the purely s -channel contribution of Fig. 9 for $q\bar{q} \leftrightarrow q\bar{q}$ to the collision term C for a hard quark, plotted as $dC/d\sqrt{s}$ vs. \sqrt{s} . The dot-dash line shows the dependence if $m_{\text{eff},q}$ and $m_{\text{eff},g}$ are both set to zero.

u -channel internal propagators but not in s -channel ones. This is the approach presented in section III. The dot-dash line hiding under the peak in Fig. 10 and smoothly decreasing at small s illustrates the result of this prescription for s -channel processes.

There are alternative possibilities which are equally valid at leading order. For example, one could include HTL self-energies multiplied by the step function $\Theta(Q^2)$ on all internal lines in $2 \leftrightarrow 2$ processes, so that they only affect spacelike propagators. With external particles treated as massless, this would also avoid double-counting mistakes. But attempting to “improve” the effective theory by including both medium-dependent self-energies on internal lines and dispersion corrections on external lines is simply wrong — unless the contributions from $2 \leftrightarrow 2$ processes degenerating into two independent scatterings are carefully separated and subtracted. Although this could be done consistently, it is needlessly complicated compared to the simple approach of treating external lines as massless and only inserting medium-dependent self-energies where they are truly required.

B. Additional scattering processes

One may wonder if any additional scattering processes need to be included in a leading-order effective theory. To examine this, first note that processes whose rates are parametrically slower than hard $2 \leftrightarrow 2$ or $1 \leftrightarrow 2$ processes will have negligible (*i.e.*, subleading in

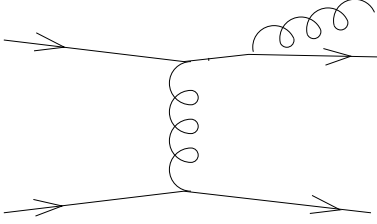


FIG. 11: A subleading hard $qq \rightarrow qqq$ process.

$g)$ effect on the dynamics of a quasiparticle. For example, consider adding an additional radiated gluon to a *hard* (*i.e.*, large momentum transfer) $2 \leftrightarrow 2$ scattering process. The case of $qq \rightarrow qqq$ is illustrated in Fig. 11. In the context of high-energy collisions in vacuum, it is well-known that bremsstrahlung gluons cost a factor of g^2 times logarithms associated with collinear and soft infrared enhancements. Soft gluon emission is unimportant for our leading-order effective theory which only describes the dynamics of hard quasiparticles. And in any case, sensitivity to small gluon momenta will be cut off in a medium by the effective mass of the gluon. Collinear logarithms will similarly be cut off by the effective masses of the quark and gluon. However, in a medium there is also a $[1+f_g]$ final state statistical factor associated with the radiated gluon. This factor can be parametrically large. But, as discussed in section IC, our assumptions limit distribution functions to be small compared to $O(g^{-2})$ for $p \gtrsim m_{\text{eff}}$. The upshot is that each radiated gluon suppresses the transition rate by a factor that is parametrically small. [If we focus on bremsstrahlung of hard gluons, then condition (1.15) implies the suppression is at least $g^{2\alpha}$, possibly times logs of $1/g$.] Therefore, a primary quark or gluon will experience a parametrically large number of hard scatterings without gluon bremsstrahlung before it undergoes one with bremsstrahlung.

The simple fact that a process is suppressed compared to others does not automatically make it irrelevant at leading order. For instance, $2 \leftrightarrow 2$ scattering does not change the total number of hard quasiparticles. Correctly including the dominant number changing processes, even if they are parametrically slow compared to the large angle scattering time, is necessary for a leading-order calculation of physics that depends on equilibration in the number of quasiparticles (such as bulk viscosity).³² However, bremsstrahlung from hard $2 \leftrightarrow 2$ scattering is not the fastest number changing process.

The most likely scattering events (as discussed in section IA) are soft scatterings with momentum transfer of order m_{eff} . The relative suppression for radiated bremsstrahlung gluons is the same as above (up to logarithms) and is at least $g^{2\alpha}$ for hard bremsstrahlung gluons. That is, an excitation will experience a parametrically large number of soft scatterings unaccompanied by hard gluon bremsstrahlung before it undergoes a soft scattering with bremsstrahlung. And soft scattering with single bremsstrahlung is the fastest number-changing process (illustrated in Fig. 3) for hard particles. Fortunately, this process has already been included in our effective kinetic theory. It is part of the $N + 1 \rightarrow N + 2$ processes which have been summed up in our effective “ $1 \leftrightarrow 2$ ” near-collinear transition rates.³³

³² This is discussed at some length, in the context of bulk viscosity for scalar theory, in Refs. [23, 24].

³³ Recall that bremsstrahlung gluons are dominated by angles less than or order of the deflection angle in the underlying $2 \rightarrow 2$ scattering event. Diagrammatically, this occurs because of cancellations between

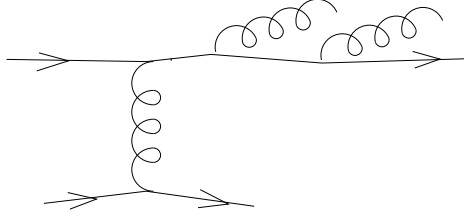


FIG. 12: A diagram contributing to double gluon bremsstrahlung.

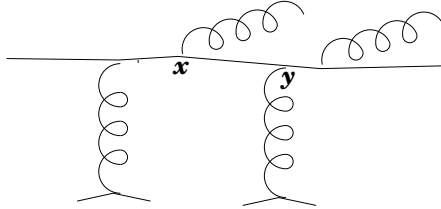


FIG. 13: Double gluon bremsstrahlung with additional soft scattering.

The basic point is that a hard scattering accompanied by bremsstrahlung does not change the distributions of quarks or gluons in any way which is distinct from the much more rapid effects of hard $2 \leftrightarrow 2$ scatterings together with soft scattering accompanied by gluon bremsstrahlung. In contrast, a soft scattering accompanied by gluon bremsstrahlung cannot be neglected, both because it changes particle number and because a single scattering of this type can produce an $O(1)$ change in the momentum of an excitation (unlike the more rapid $2 \leftrightarrow 2$ soft scatterings) at a rate which can be competitive with hard $2 \leftrightarrow 2$ scattering.

To make the above discussion more concrete, let us briefly specialize to typical excitations in near-equilibrium systems. In that case, the rate of hard scattering with hard gluon bremsstrahlung is $O(g^6 T)$, which is $O(g^2)$ suppressed relative to the $O(g^4 T)$ rate of hard $2 \leftrightarrow 2$ processes. The rate of soft scattering with hard bremsstrahlung is $O(g^4 T)$, which is $O(g^2)$ suppressed relative to the $O(g^2 T)$ rate of straight $2 \leftrightarrow 2$ soft scattering.

As a further example of the suppression of higher-order processes, consider soft $2 \leftrightarrow 2$ scattering with hard double bremsstrahlung, as depicted in Fig. 12, which we might call a “ $1 \leftrightarrow 3$ ” splitting. As already discussed, this would be suppressed by $g^{2\alpha}$ compared to single bremsstrahlung. It is therefore irrelevant at leading order, since a parametrically large number of “ $1 \leftrightarrow 2$ ” single bremsstrahlung events will occur for every one of these double bremsstrahlung events. [Near equilibrium, the rate for this “ $1 \leftrightarrow 3$ ” double bremsstrahlung is $g^6 T$, compared to the $g^4 T$ rate of “ $1 \leftrightarrow 2$ ” processes.]

Now consider adding one or more additional scatterings to the double bremsstrahlung process, to generate a diagram like the one shown in Fig. 13. Adding additional soft scatterings can increase the cross-section, because the internal line running from x to y in the

different diagrams, such as those of Fig. 3. But it can also be seen by reviewing classical formulas for the intensity of bremsstrahlung radiation. Since the momentum transfer of the most prevalent collisions is order m_{eff} , the deflection angle is order $m_{\text{eff}}/p_{\text{primary}}$ for a primary excitation. In local equilibrium settings, this is order g .

figure can go on shell.³⁴ This part of the amplitude, however, really represents two consecutive “ $1 \leftrightarrow 2$ ” processes and so is already accounted for. The process of Fig. 13 differs significantly from two consecutive collisions only when the time between x and y is comparable to the duration ($1/g^2 T$ near equilibrium) of the individual “ $1 \leftrightarrow 2$ ” processes. In momentum space, that corresponds to the kinematic region where that propagator is just as off-shell in energy as the intermediate quark line in the double bremsstrahlung, single soft scattering case of Fig. 12 considered previously. In other words, there is no additional on-shell enhancement except when the process degenerates into separate scattering events, which are already included in the effective kinetic theory.

In summary, multiple gluon bremsstrahlung processes are either indistinguishable from a sequence of “ $1 \leftrightarrow 2$ ” and $2 \leftrightarrow 2$ processes or else are parametrically slower and do not accomplish any relevant relaxation not already provided by a sequence of faster processes. After examining these, and other possibilities, we are unaware of any processes which can affect reasonable observables at leading order in g , beyond those which have already been included in our effective theory.³⁵

C. Effective kinetic theory beyond leading order?

Typical effective theories (such as heavy quark theory, or non-relativistic QED) can be systematically improved order-by-order in powers of the ratio of scales which underlies the effective theory. Having constructed a leading-order effective kinetic theory for the dynamics of a hot gauge theory, it is natural to ask whether one can formulate a beyond-leading-order kinetic theory which will correctly incorporate relative corrections suppressed by one or more powers of g . This is an interesting open question.

Consider, for simplicity, the case of systems which differ from equilibrium by at most $O(1)$, so that all relevant hard momenta are $O(T)$. Any attempt to construct an effective theory of hot dynamics beyond leading order must handle numerous different sources of subleading corrections. These include:

1. Kinematic mass corrections of order $m_{\text{eff}}^2/p_{\text{hard}}^2 \sim g^2$. These are everywhere: in the convective derivative of the Boltzmann equation, in the overall kinematics of the collision terms, inside the effective $2 \leftrightarrow 2$ scattering amplitudes, etc. Consistently including

³⁴ For comparison, the internal quark lines in the double bremsstrahlung process of Fig. 12 have virtualities $P^2 \sim m_{\text{eff}}^2$ since the angle between each hard gluon and the emitting quark line is $O(m_{\text{eff}}/p_{\text{primary}})$. (See the previous footnote.) Hence these internal lines are off-shell in energy by an amount of order $P^2/E \sim m_{\text{eff}}^2/p_{\text{primary}}$ (or $g^2 T$ in the near-equilibrium case). These internal lines are prevented from being more on-shell by the medium-dependent effective masses of particles.

³⁵ This assertion does deserve a few caveats. Since QCD exactly conserves the net fermion number in each flavor, but weak interactions do not, weak interaction collision terms cannot be neglected if one is interested in the evolution of flavor asymmetries on sufficiently long time scales. Similarly, in hot electroweak theory explicit baryon production/destruction terms representing the effects of non-perturbative baryon number changing processes can be relevant on time scales large compared to the mean free times of processes discussed in this paper. See Ref. [2] for more discussion of these points.

such corrections should be feasible, but will force one to separate and subtract the degenerating parts of scattering rates, as discussed in section VI A.

2. Contributions from higher order tree processes, such as bremsstrahlung from hard scattering. Numerous such additional processes appear at $O(g^2)$ and would need to be included in the collision terms, again with appropriate care to eliminate phase space regions where an intermediate line goes on-shell and the process separates into multiple scattering events.
3. Loop corrections to $2 \leftrightarrow 2$ effective scattering amplitudes. For hard scattering, these will be order g^2 effects, but for soft scattering, the relevant loop expansion parameter is g , not g^2 . Also, the HTL approximation to the self-energies required in soft exchange processes receive $O(g)$ corrections because of kinematic approximations made in the HTL results.
4. Subleading corrections to effective near-collinear transition rates, and a proper treatment of the soft emission region. We believe these enter at $O(g)$. Evaluating such corrections would require a next-to-leading order treatment of LPM suppression. This is unknown territory.
5. Contributions from soft ($\mathbf{p} \sim gT$) on-shell excitations. The size of such contributions depends on the sensitivity of observables of interest to soft momenta. For observables like fermion current densities or the traceless part of the stress tensor (whose behaviors determines diffusion constants and shear viscosity), soft contributions are suppressed by $O(g^4)$ or more. Incorporating soft contributions requires formulating a kinetic theory which correctly describes both hard (ultrarelativistic) and soft (non-relativistic) excitations.
6. Contributions from non-perturbative gauge field dynamics on the g^2T (ultrasoft) scale. The importance of very small angle scattering via ultrasoft gauge boson exchange is suppressed, relative to soft exchange, by g^2 ; so we expect ultrasoft physics effects to enter as g^2 corrections to our effective kinetic theory. This means that nonperturbative inputs will be necessary to formulate a kinetic theory which correctly describes $O(g^2)$ corrections. We have no idea how this could be done in practice.
7. Corrections due to the uncertainty in energy of excitations. The relative size of such corrections is controlled by the inverse of an excitation's energy times its mean free time between scatterings. For soft scatterings of hard excitations, this is $O(g^2)$. Correctly incorporating such quantum corrections to kinetic theory is an interesting open problem.

Consistently incorporating $O(g)$ corrections may well be feasible, but extending the effective kinetic theory to include $O(g^2)$ effects involves major conceptual challenges as well as technical difficulty.

Acknowledgments

This work was supported, in part, by the U.S. Department of Energy under Grant Nos. DE-FG03-96ER40956 and DE-FG02-97ER41027.

APPENDIX A: ISOTROPIC DISTRIBUTIONS

Isotropic (rotationally invariant) distributions represent a physically interesting class of problems intermediate between completely general non-equilibrium systems on one hand, and equilibrium or near-equilibrium systems on the other. It is widely appreciated that substantial simplifications occur for equilibrium systems. For isotropic systems, almost as high a level of simplification is possible. The following results are written in the plasma rest frame, which is uniquely defined for an isotropic system.

We begin with the retarded fermion self-energy $\Sigma_{\text{Ret}}(K) = \gamma_\mu \Sigma_{\text{Ret}}^\mu(K)$, for soft 4-momentum $K \equiv (k^0, \mathbf{k})$ such that $k^0 \sim \sqrt{\mathbf{k}^2} \equiv k \ll p_{\text{screen}}$. With isotropic distributions, this soft self-energy has exactly the same structure as in equilibrium [25, 26],

$$\Sigma^0(K) = \frac{m_{\text{eff,f}}^2}{4k} \left[\ln \left| \frac{k^0+k}{k^0-k} \right| - i\pi \Theta(k^2 - (k^0)^2) \right], \quad (\text{A1})$$

$$\Sigma^i(K) = -\mathbf{k}^i \frac{m_{\text{eff,f}}^2}{2k^2} \left\{ 1 - \frac{k^0}{2k} \left[\ln \left| \frac{k^0+k}{k^0-k} \right| - i\pi \Theta(k^2 - (k^0)^2) \right] \right\}. \quad (\text{A2})$$

The overall coefficient $m_{\text{eff,f}}^2$ is given by the integral (4.10) which determines the effective mass for hard fermions. In the literature, this self-energy is more conventionally written in terms of $M_q^2 \equiv \frac{1}{2}m_{\text{eff,f}}^2$, because M_q is then the frequency of oscillation for a $\mathbf{k} = 0$ fermion.

The case of the retarded gauge field self-energy $\Pi_{\text{Ret}}(K)$ is similar. As in thermal equilibrium [27, 28], the self-energy can be decomposed into longitudinal and transverse pieces,

$$\Pi_{\text{Ret}}^{\mu\nu}(K) = \Pi_{\text{T}}(K) P^{\mu\nu}(K) + \Pi_{\text{L}}(K) Q^{\mu\nu}(K), \quad (\text{A3})$$

with

$$P^{\mu\nu}(K) = \eta^{\mu\nu} + u^\mu u^\nu - \frac{\mathbf{k}^\mu \mathbf{k}^\nu}{k^2}, \quad (\text{A4})$$

$$Q^{\mu\nu}(K) = \frac{(k^2 u^\mu + k^0 \mathbf{k}^\mu)(k^2 u^\nu + k^0 \mathbf{k}^\nu)}{k^2 [(k^0)^2 - k^2]}. \quad (\text{A5})$$

Here $\mathbf{k}^\mu \equiv K^\mu + u^\mu u \cdot K = (0, \mathbf{k})$ denotes the part of the 4-momentum K orthogonal to the rest frame 4-velocity u . The projectors $P^{\mu\nu}$, $Q^{\mu\nu}$, and $K^\mu K^\nu / K^2$ are mutually orthogonal and sum to the metric, $P^{\mu\nu} + Q^{\mu\nu} + K^\mu K^\nu / K^2 = \eta^{\mu\nu}$. The transverse and longitudinal self-energies are

$$\Pi_{\text{T}}(K) = m_{\text{eff,g}}^2 \left\{ \frac{(k^0)^2}{k^2} + \frac{k^0(k^2 - (k^0)^2)}{2k^3} \left[\ln \left| \frac{k^0+k}{k^0-k} \right| - i\pi \Theta(k^2 - (k^0)^2) \right] \right\}, \quad (\text{A6})$$

$$\Pi_{\text{L}}(K) = 2m_{\text{eff,g}}^2 \frac{k^2 - (k^0)^2}{k^2} \left\{ 1 - \frac{k^0}{2k} \left[\ln \left| \frac{k^0+k}{k^0-k} \right| - i\pi \Theta(k^2 - (k^0)^2) \right] \right\}, \quad (\text{A7})$$

where $m_{\text{eff,g}}^2$ is the asymptotic gluon mass defined in Eq. (4.6). Equivalent forms in the literature are more commonly written in terms of the leading order Debye mass $m_{\text{D}}^2 = 2m_{\text{eff,g}}^2$, or occasionally in terms of the leading order plasma frequency $\omega_{\text{pl}}^2 = m_{\text{D}}^2/3$. Note that the definition of Π_{L} is not uniform in the literature (even in previous work by the authors of the present paper!). The above notation agrees with that of Weldon [28]. The other common usage is that of Braaten and Pisarski [29], who define Π_{L} to be $-k^2/K^2$ times our value, so that $\Pi_{\text{L}}^{(\text{Braaten-Pisarski})} = -\Pi_{\text{Ret}}^{00}$.

Rotational symmetry, even in the absence of equilibrium, is sufficient to derive a relation between the imaginary part of the retarded self-energy and the Wightman self-energy, at soft momenta. Namely,

$$\Pi_{12}^{\alpha\beta}(K) = -\frac{2T_*}{k^0} \operatorname{Im} \Pi_{\text{Ret}}^{\alpha\beta}(K), \quad (\text{A8})$$

where

$$T_* \equiv \sum_s \nu_s \frac{g^2 C_s}{d_A} \mathcal{I}_s \Big/ \sum_s \nu_s \frac{g^2 C_s}{d_A} \mathcal{J}_s, \quad (\text{A9})$$

and \mathcal{I}_s and \mathcal{J}_s are the integrals defined in Eqs. (1.7) and (1.6), evaluated with the distribution function for species s . Relation (A8) is just the small frequency form of the equilibrium fluctuation-dissipation relation (5.9), but with the equilibrium temperature replaced by T_* .

Consequently, the Wightman correlation function, for soft momenta, is merely a rescaled version of the thermal Wightman correlation function,

$$\langle\langle A_\mu(K)[A_\nu(K)]^* \rangle\rangle \Big|_{\substack{\text{non-eq.} \\ \text{isotropic}}} = \frac{T_*}{T_{\text{eff}}} \langle\langle A_\mu(K)[A_\nu(K)]^* \rangle\rangle \Big|_{\substack{\text{equil.} \\ T=T_{\text{eff}}}}, \quad (\text{A10})$$

at the temperature T_{eff} for which the equilibrium Debye mass coincides with the correct effective Debye mass,³⁶ $m_D^2(T_{\text{eff}})|_{\text{equil.}} = 2m_{\text{eff,g}}^2$. Note that the value of T_* is not in general the same as T_{eff} .

Relation (A10) permits one to use recent results of Aurenche *et al.* [30] to reduce the four dimensional integral involving the Wightman correlator appearing in the integral equation (5.3) down to a two dimensional integral over transverse momenta. One may show that

$$\begin{aligned} & g^2 \int \frac{d^4 Q}{(2\pi)^4} 2\pi \delta(v_{\hat{n}} \cdot Q) v_{\hat{n}}^\mu v_{\hat{n}}^\nu \langle\langle A_\mu(Q)[A_\nu(Q)]^* \rangle\rangle \Big|_{\substack{\text{non-eq.} \\ \text{isotropic}}} h(\mathbf{q}_\perp) \\ &= g^2 T_* \int \frac{d^2 \mathbf{q}_\perp}{(2\pi)^2} \left(\frac{1}{\mathbf{q}_\perp^2} - \frac{1}{\mathbf{q}_\perp^2 + m_D^2} \right) h(\mathbf{q}_\perp), \end{aligned} \quad (\text{A11})$$

where $h(\mathbf{q}_\perp)$ is any function of \mathbf{q}_\perp .

³⁶ Explicitly, for an $SU(N_c)$ theory with N_f fundamental Dirac fermions, $\frac{1}{6}(N_c + N_f C_F d_F/d_A) g^2 T_{\text{eff}}^2 = m_{\text{eff,g}}^2$.

APPENDIX B: RELATIONSHIP OF $d\Gamma_g/d^3k$ TO γ_{bc}^a

The leading-order equilibrium differential rate for production for hard gluons, as defined in Ref. [8], corresponds to the gain part of gluon collision terms (2.2) and (2.7), evaluated in equilibrium and multiplied by $\nu_g/(2\pi)^3$. Explicitly, the near-collinear LPM-suppressed part of the production rate for hard gluons with momentum $\mathbf{k} = k\hat{\mathbf{n}}$ is, at leading order,

$$\begin{aligned} \frac{d\Gamma_g^{\text{LPM}}}{d^3k} &= \frac{1}{4\pi k^2} \frac{d\Gamma_g^{\text{LPM}}}{dk} \\ &= \frac{[1+n_b(k)]}{k^2} \left(\frac{1}{2} \int_0^\infty dp dp' \delta(p'+p-k) \gamma_{gg}^g(k\hat{\mathbf{n}}; p'\hat{\mathbf{n}}, p\hat{\mathbf{n}}) n_b(p') n_b(p) \right. \\ &\quad + \int_0^\infty dp dp' \delta(p'-p-k) \gamma_{gg}^g(p'\hat{\mathbf{n}}; p\hat{\mathbf{n}}, k\hat{\mathbf{n}}) n_b(p') [1+n_b(p)] \\ &\quad + N_f \int_0^\infty dp dp' \delta(p'+p-k) \gamma_{q\bar{q}}^g(k\hat{\mathbf{n}}; p'\hat{\mathbf{n}}, p\hat{\mathbf{n}}) n_f(p') n_f(p) \\ &\quad \left. + 2N_f \int_0^\infty dp dp' \delta(p'-p-k) \gamma_{q\bar{q}}^g(p'\hat{\mathbf{n}}; p\hat{\mathbf{n}}, k\hat{\mathbf{n}}) n_f(p') [1-n_f(p)] \right). \quad (\text{B1}) \end{aligned}$$

The $\frac{1}{2}$ in the first term is an initial-state symmetry factor, the 2 multiplying the final term reflects the identical contributions from $q \rightarrow qg$ and $\bar{q} \rightarrow \bar{q}g$, and N_f is the number of Dirac fermion flavors. $n_b(\omega)$ and $n_f(\omega)$ are equilibrium Bose and Fermi distribution functions, respectively. Ref. [8] expresses results more compactly by using crossing symmetries. For a more direct comparison with that paper, expression (B1) can be rewritten as

$$\begin{aligned} \frac{d\Gamma_g^{\text{LPM}}}{d^3k} &= \frac{[1+n_b(k)]}{k^2} \left(\frac{1}{2} \int_{-\infty}^\infty dp dp' \delta(p'-p-k) \gamma_{gg}^g(p'\hat{\mathbf{n}}; p\hat{\mathbf{n}}, k\hat{\mathbf{n}}) n_b(p') [1+n_b(p)] \right. \\ &\quad \left. + N_f \int_{-\infty}^\infty dp dp' \delta(p'-p-k) \gamma_{q\bar{q}}^g(p'\hat{\mathbf{n}}; p\hat{\mathbf{n}}, k\hat{\mathbf{n}}) n_f(p') [1-n_f(p)] \right). \quad (\text{B2}) \end{aligned}$$

However, the authors of Ref. [8] should be profoundly chastised for not pointing out that this differential gluon production rate is, in fact, an infrared divergent quantity. The problem arises from the $p \rightarrow 0$ region of the $g \leftrightarrow gg$ term in (B2). This portion of the integral represents processes in which a hard gluon with momentum \mathbf{p}' nearly equal to \mathbf{k} experiences a soft scattering with emission or absorption of a soft gluon to yield a hard gluon with momentum \mathbf{k} . But physical quantities can only depend on this production rate minus the corresponding rate at which gluons are scattered out of the mode \mathbf{k} , and the infrared sensitivity cancels in the difference of these rates. In other words, although the production rate $d\Gamma_g^{\text{LPM}}/d^3k$ is not actually well-defined, the complete collision terms (2.7) built from the same near-collinear transition amplitudes are infrared safe.

[1] H. Heiselberg, Phys. Rev. **D49**, 4739 (1994) [hep-ph/9401309].

[2] P. Arnold, G. D. Moore and L. G. Yaffe, JHEP **0011**, 001 (2000) [hep-ph/0010177].

[3] R. Baier, A. H. Mueller, D. Schiff and D. T. Son, Phys. Lett. B **502**, 51 (2001) [hep-ph/0009237].

[4] P. Arnold, D. T. Son and L. G. Yaffe, Phys. Rev. D **59**, 105020 (1999) [hep-ph/9810216].

[5] A. Selikhov and M. Gyulassy, Phys. Lett. B **316**, 373 (1993) [nucl-th/9307007].

[6] D. Bodeker, Phys. Lett. B **426**, 351 (1998) [hep-ph/9801430].

[7] D. Bodeker, Nucl. Phys. B **559**, 502 (1999) [hep-ph/9905239].

[8] P. Arnold, G. D. Moore and L. G. Yaffe, JHEP **0206**, 030 (2002) [hep-ph/0204343].

[9] P. Arnold, G. D. Moore and L. G. Yaffe, JHEP **0111**, 057 (2001) [hep-ph/0109064].

[10] P. Aurenche, F. Gelis, R. Kobes and H. Zaraket, Phys. Rev. D **58**, 085003 (1998) [hep-ph/9804224].

[11] P. Arnold, G. D. Moore and L. G. Yaffe, JHEP **0112**, 009 (2001) [hep-ph/0111107].

[12] R. Snider in *Lecture Notes in Physics*, vol. 31: *Transport Phenomena* (Springer, 1974), ed. J. Ehlers *et al.*

[13] S. Mrówczyński, Phys. Lett. B **393**, 26 (1997) [hep-ph/9606442].

[14] B. L. Combridge, J. Kripfganz and J. Ranft, Phys. Lett. **B70**, 234 (1977).

[15] S. Mrówczyński and M. H. Thoma, Phys. Rev. D **62**, 036011 (2000) [hep-ph/0001164].

[16] M. E. Carrington, D. f. Hou and M. H. Thoma, Eur. Phys. J. C **7**, 347 (1999) [hep-ph/9708363].

[17] E. M. Lifshitz and L. P. Pitaevskii, *Physical Kinetics* (Pergamon, 1981).

[18] P. Arnold, D. T. Son and L. G. Yaffe, Phys. Rev. D **59**, 105020 (1999) [hep-ph/9810216].

[19] F. Gelis, hep-ph/0209072.

[20] M. Gyulassy and X. n. Wang, Nucl. Phys. B **420**, 583 (1994) [nucl-th/9306003].

[21] S. Klein, Rev. Mod. Phys. **71**, 1501 (1999) [hep-ph/9802442].

[22] L. D. Landau and I. Pomeranchuk, Dokl. Akad. Nauk Ser. Fiz. **92** 535 (1953); *ibid.* **92** 735 (1953). These papers are also available in English in L. Landau, *The Collected Papers of L.D. Landau* (Pergamon, New York, 1965).

[23] S. Jeon, Phys. Rev. D **52**, 3591 (1995) [hep-ph/9409250].

[24] S. Jeon and L. G. Yaffe, Phys. Rev. D **53**, 5799 (1996) [hep-ph/9512263].

[25] V. V. Klimov, Sov. J. Nucl. Phys. **33**, 934 (1981) [Yad. Fiz. **33**, 1734 (1981)].

[26] H. A. Weldon, Phys. Rev. D **26**, 2789 (1982).

[27] O. K. Kalashnikov and V. V. Klimov, Sov. J. Nucl. Phys. **31**, 699 (1980) [Yad. Fiz. **31**, 1357 (1980)].

[28] H. A. Weldon, Phys. Rev. D **26**, 1394 (1982).

[29] E. Braaten and R. D. Pisarski, Nucl. Phys. B **337**, 569 (1990).

[30] P. Aurenche, F. Gelis and H. Zaraket, JHEP **0205**, 043 (2002) [hep-ph/0204146].